THE UNIVERSITY OF MICHIGAN

COLLEGE OF ENGINEERING

Department of Chemical and Metallurgical Engineering

Progress Report

AN INVESTIGATION OF METAL SPINNING

B. Avitzur S. Floreen E. E. Hucke D. V. Ragone

UMRI Project 2621

under contract with:

SPINCRAFT, INC.
MILWAUKEE, WISCONSIN

Ref.: Contract No. DA-11-022-ORD-2542
Army Ballistic Missile Agency

administered by:

THE UNIVERSITY OF MICHIGAN RESEARCH INSTITUTE· ANN ARBOR

March 1959

TABLE OF CONTENTS

List of Tables iv
List of Figures v
Abstract 1
Objective 1
I. Introduction 2
A. The Process, General Description 3
B. The Procedure 5
1. The Analytical Solution 8
2. The Experimental Verification 9
II. Nomenclature 10
III. The Analytical Approach 13
A. The Process 13
B. The Process Variables 17
C. The Velocity Field 20
D. The Strain-Rates Field 23
E. The State of Stress 25
F. The Power 27
IV. Mathematical Description of the Process 30
A. The Sets of Axis and Their Transformation 30
B. The Roller 32
C. The Cone 33
D. The Area of Contact 36
V. Solving the Power by the Deformation Theory 45
VI. Simplifying the Equations for Numerical Evaluation 49
A. Integrating the Power 50
B. Computing the Partial Power 52
C. Computing the Complementary Power 52
D. Evaluating the Strain-Rates Ratio ζ 55
VII. The Tangential Force 57
VIII. The Experimental Work 60
A. The Experimental Determination of the Nature of Deformation 60
B. Measuring the Power and Tangential Force 65
IX. The Results 70
X. Conclusions 72
XI. References 80
Appendices
1. Program for the IBM 650 Digital Computer 81
2. Comparing the Tangential Force for Shear and Bending 98
3. Evaluating the Yield Limit 101

LIST OF TABLES

Table		
I - Directional Cosines	30	
II - Assignment List for the Results	86	
III - General Assignment List	87	
IV - Identification Number (10) Key	91	
V - Distortion of Holes Pattern in Spun Cones	64	
VI - Cincinnati Results of Recorded Forces	67	
VII - Computed Weighted Power and Tangential Force		under separate cover
VIII - The Distribution of Strain Rates and $\dot{\varepsilon}$		under separate cover

LIST OF FIGURES

Figure			Page
1	-	The Cone and Mandrel	4
2	-	The Roller	6
3	-	The Positioning of the Roller	7
4	-	The Process	14
5	-	The Deformation	15
6	-	Disc Analogy	16
7	-	Displacing the Disc	18
8	-	Viscous Flow Around an Obstacle	21
9	-	The Zones of the Cone	35
10	-	The Area of Contact	35
11	-	Line BC	38
12	-	The Boundary CDEF	48
13	-	Feed Marks	49
14	-	Approximating the Torus by a Cylinder	54
15	-	Approximated Area of Contact	82
16	-	Holes in the Original Disc	62
17	-	A Cut of a Spun Cone	63
18	-	Directions of Holes in the Cone	66
19	-	The Shear and Bending Strains	99
20	-	Comparing Shear Deformation to Bending	102
21	-	Tangential Force vs Feed	76
22	-	Tangential Force vs Included Angle	77
23	-	Tangential Force vs "Round-off" Radius	78
24	-	Tangential Force vs Roller's Radius	79
25	-	Spincraft Experimental Set Up	68
26	-	Specimen for Tensile Test	71
27	-	Flow Diagram for Computer Program	92
28	-	Stress Strain Curve	104

ABSTRACT

The cone, the roller, and the geometry of the operation are described mathematically. A shear type of deformation is postulated, based on experimental evidence. The displacements, velocities, strain rates, and stress fields are computed for "Mises Material," and hence with Mises stress-strain rate law. The power consumed in the operation is computed from the strain rates and stress fields. The expression for the power is in a form that cannot be solved analytically. A numerical solution is therefore presented in graphical form, where the power and tangential force are plotted for a variety at process variables. The numerical solution is compared with actual measured power and forces.

OBJECTIVE

The purpose of this study is to relate the power requirement and the tangential force for mechanical spinning of cones to the process variables.

INTRODUCTION

The aim of this study is to help toward better understanding of the process of spinning, and to develop a method for prediction of the power requirements. The power consumed in the process is of interest for the design of new equipment, for intelligent choice of the best machine for the job, and for the right choice of the process variables for a specified job. Furthermore, this power is the predominant factor dictating the interaction force between the roller and the cone. Therefore it can be later utilized for the determination of the forces.

Spinning is a metal-shaping process widely used to fabricate pieces having rotational symmetry. In common spinning practice, a pattern having the final shape of the desired piece is mounted on a lathe. A flat sheet of metal is then clamped to the pattern, and while the pattern and sheet are revolving, the sheet is forced back over the pattern by pressing against the sheet with some type of spinning tool. Reduction in thickness of the sheet may or may not take place. Generally the spinning tool is a roller or a heavy wooden stick.

The process can be done by hand when the spinning is done by a skilled craftsman who knows by experience how to lay the sheet against the pattern; or it can be done mechanically, in which case the forces are applied by some mechanical system.

Many shapes and sizes can be spun; pieces up to 10 feet in diameter are common. Because of the nature of the process, very large reductions in thickness, up to 75% per pass in some cases, can be achieved. With suitable

equipment it is also possible to hot-spin. There do not seem to be any restrictions as to deformable materials which can be spun. Aluminum, brass, stainless steel, titanium, and super-alloys, for example, have all been successfully spun.

Because of the simplicity of the operation, spinning offers some distinct economical advantages. Lenbridge[1] has shown that spinning is more economical for producing a small number of pieces than deep drawing because of the low setup time and costs. The pattern used for spinning, for example, can often be made of wood, which saves a great deal of tooling expense.

This study deals with the mechanical spinning of cones. It does not pertain to the "formability" problem but it does deal with the effect of the process variables on the power and tangential force for successful operation, where the variables are within their permissible range.

A. THE PROCESS, GENERAL DESCRIPTION

The raw material is a disc of diameter D and uniform thickness S_o. The disc is mounted on a circular conical mandrel, which is clamped to the head of the spinning machine, and rotated. A forming roller is driven on tracks on the bed of the machine parallel to the side of the mandrel. The outer diameter D_1 of the cone (Fig. 1) remains the same as the original diameter of the disc. The cone's thickness is now:

$$S_1 = S_o \operatorname{Sin} \alpha_o$$

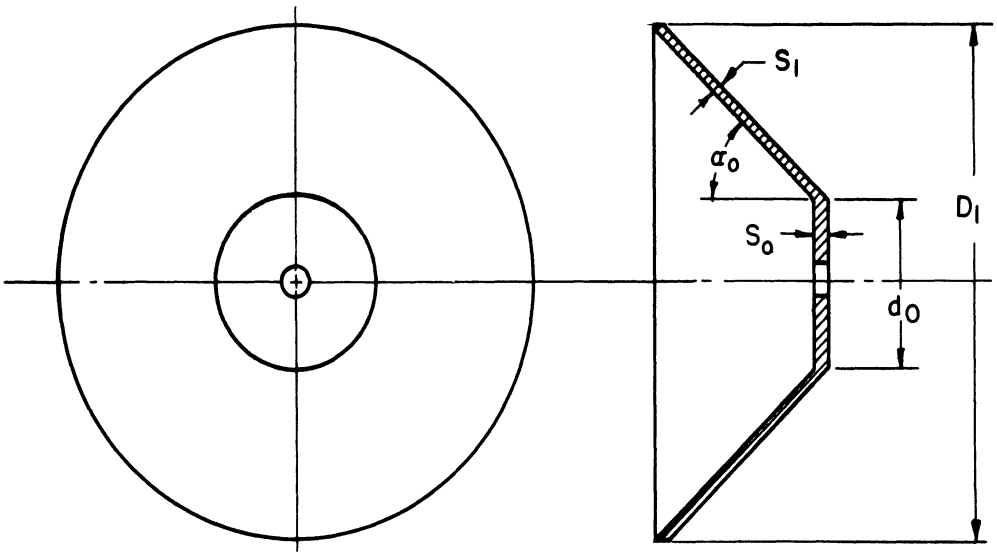

THE FINISHED CONE

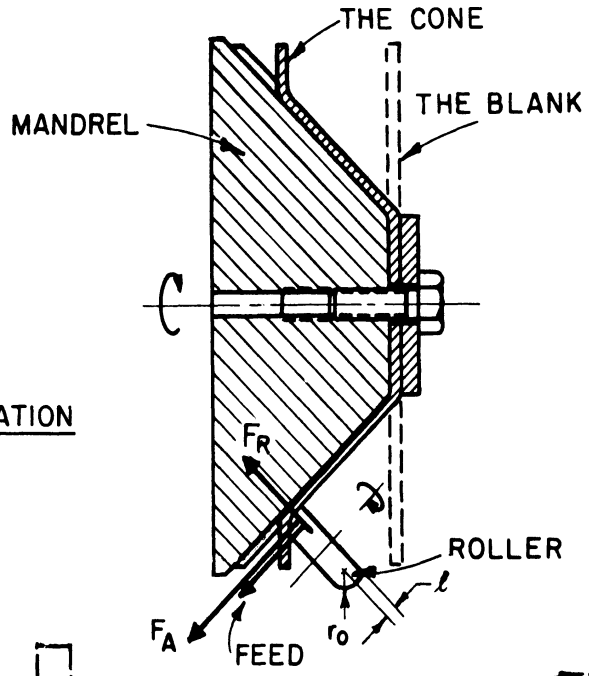

THE OPERATION

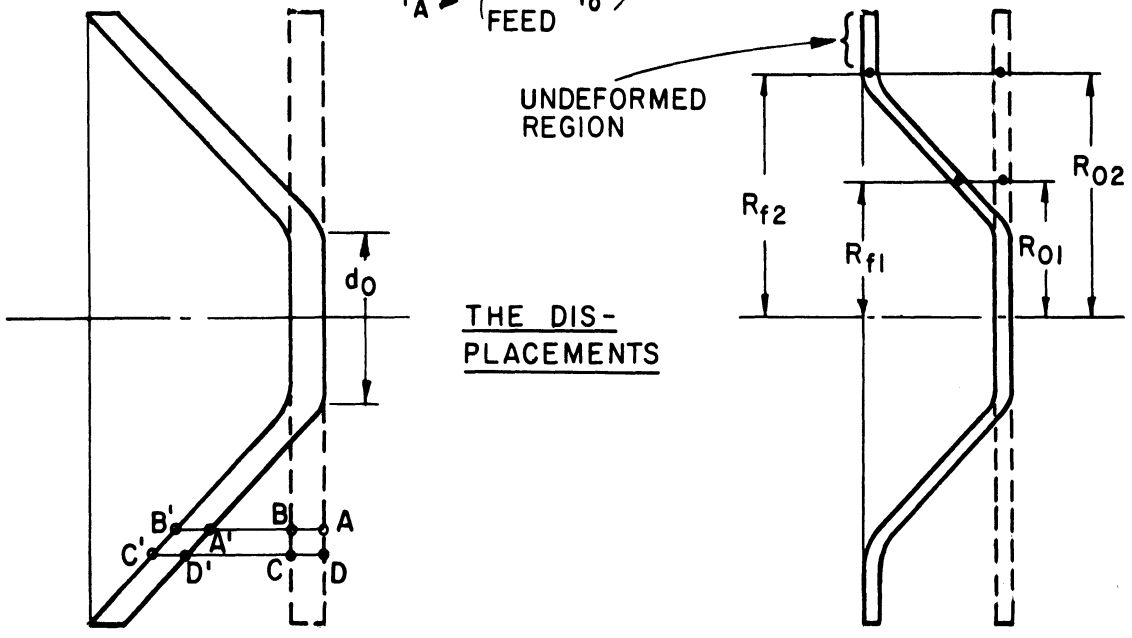

THE DIS-PLACEMENTS

Fig. 1 - The cone

This type of spinning is called by different names like forming, hydro-spinning, etc. Later on the displacements and strains will be analyzed in more detail.

The roller is built from a hardened tool steel and mounted on a shaft with ball or roller bearings. There are many shapes of rollers; some are illustrated in Fig. 2. A common feature of all rollers is the "round-off" portion of radius r_o. When thin discs are spun with high feeds, a land is added to the roller to smooth off the feed marks. It is sometimes found convenient to add a front as in shape III of Fig. 2, to push the flange forward.

The relative position of the roller's axis to the side of the mandrel may differ much in different setups. Some examples are shown in Fig. 3.

From this variety of possibilities, a common roller (shape 1) which is oriented with its axis parallel to the side of the mandrel was chosen to be analyzed. The changes in the roller's shape and its positioning might sometimes make the difference between a successful operation or failure. However, the strains and stresses during a successful operation do not differ much from case to case.

B. THE PROCEDURE

This study can be divided into two parts: the analytical solutions, and the experimental verification.

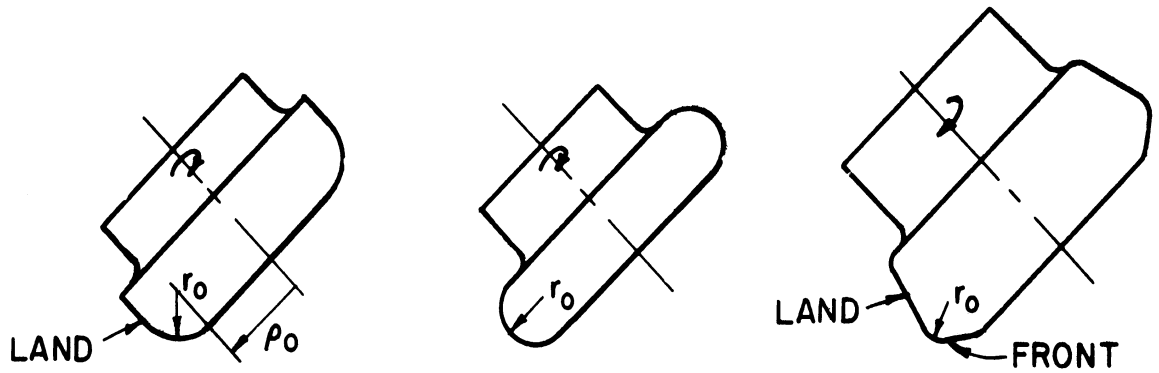

Fig. 2 - The roller

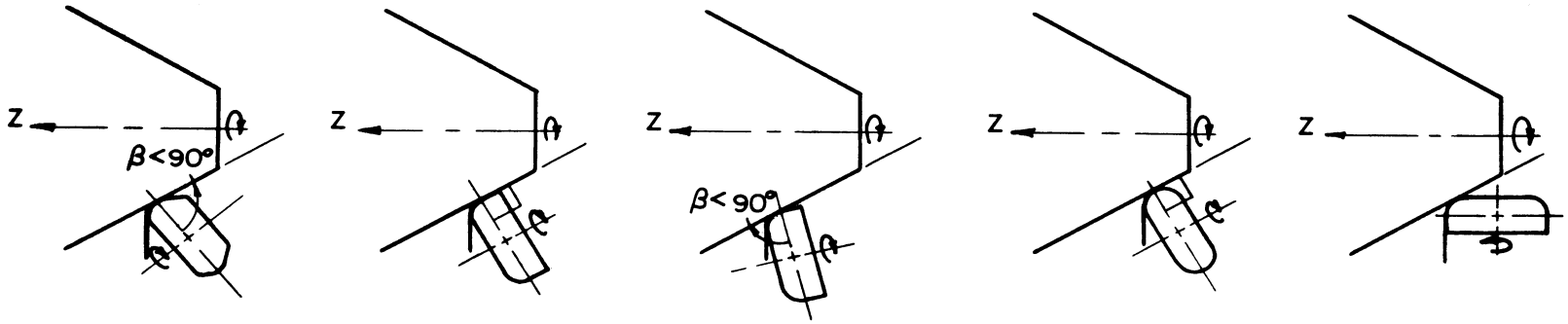

Fig. 3 - Rollers' positioning

1. The Analytical Solution

The geometry of the operation has been described mathematically. The equations of the cone and the roller have also been formulated. The boundaries of the area of contact between the roller and the cone have then been found.

A shear type of deformation has been postulated, based on experimental evidence.

Two solutions have been derived for the plastic work of deformation: one was based on the incremental theory (Mises stress-strain-rate law), the other, on the deformation theory (stress-strain law). Both solutions were computed for Mises Material, which implies:

(1) no elastic deformation, and consequently no volumetric change;

(2) no strain-hardening.

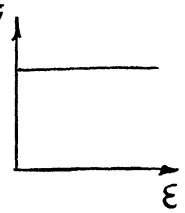

However, the deformation theory has an additional solution for the case of linear strain-hardening effect.

a. The Incremental Theory Solution. - The velocity and strain-rate fields were computed using the geometric formulation above. An expression for the plastic work of deformation was then developed. The numerical values are computed using a digital computer.

b. The Deformation Theory Solution. - The solution was simply derived by assuming that the deformation was reached by monotonically increased shear from zero to the final state in a finished cone.

2. The Experimental Verification

Two different types of experiments were conducted.

a. First Set of Experiments. - This set was designed to help choose the right type of deformations that take place during the process. Holes were drilled in the original discs and then plugged. Their direction was traced after the spinning. This series provides support for the choice of shear deformation in the analysis.

b. Second Set of Experiments. - In this set of experiments the forces and power were measured. This set was run separately in two locations. At the Cincinnati Milling Machine Co., a dynamometer was used. Three components of the spinning force were recorded. A three-dimensional dynamometer at the arm of the roller is connected to a three-channel recorder. The actual forces for a diversified set of parameters was found. At Spincraft, Inc., the power requirement for the d-c motor driving the mandrel was recorded. The power requirement for a diversified set of parameters was found.

NOMENCLATURE

X,Y,Z - Rectangular coordinate system with:
O - origin.
R,Θ,Z - Cylindrical polar coordinate system with origin O
x,y,z - Rectangular coordinate system with:
O' - origin.
$X,Y,Z,-R,\Theta,Z,-x,y,z,$ coordinates of a point in space in the corresponding coordinate system.
a_i - (where i = 1,2,3) - The three coordinates of the origin O in the x,y, z coordinates system.
b_j - (where j = 1,2,3) - The three coordinates of the origin O' in the X,Y,Z coordinates system.
a_{ij} - The directional cosines of X,Y,Z axis in the x,y,z coordinate system and vice versa.

r_o - "Round-off" radius of the roller.
ρ_o - The roller's radius.
α_o - Half the included angle of the cone; also the angle between Z and z axis.
R_o - Instantaneous radius at which the roller touches the cone.
$R_{o_{Min.}}$ - Cose's radius (R) at the bend.
$R_{o_{Max.}}$ - The blank's outer radius.
D_1 - Outer diameter of the cone.
S_o - Thickness of the blank.
S_1 - Thickness of the final cone.
σ_o - The cone's material yield limit at uniaxial tensile test.
k - Mises yield limit.

N - The speed in rpm.
F - The feed in ipr.
t - Time
t_o - Initial time
n - No. of revolutions passed from initial time.

U - Velocity in ipm.
$\bar{U}$ - Velocity vector.
U_R - Velocity in R direction in ipm.
U_Θ - Velocity in Θ direction in ipm.
U_Z - Velocity in Z direction in ipm.
U_{ZP} - Principal part of U_Z component of the velocity.
U_{ZC} - Complementary part of U_Z component of the velocity.
ΔU_{ZP} - Change in $U_{Z\rho}$.
ΔU_{ZC} - Change in U_{ZC}.

v - Velocity.

S_t - Circumferential velocity.

S_A - Feed velocity.

S_R - Radial velocity.

$\dot{R},\dot{\theta},\dot{Z}$ - Velocities in R,θ, and Z directions.

G, $G(R)$, $G(R,\theta,Z)$, $G(R,\theta,Z,n)$, etc. - The function of the "round-off" surface of the roller.

G_R, G_θ, G_Z, G_t, - The partial derivatives of G with respect to R,θ,Z and t, respectively.

$Z = H(R,\theta,n)$ - The function of the "round-off" surface expressing Z explicitly.

A,B,C,D, E, F - Points on the boundaries of the area of contact.

AB, BC, CD, DE, EF, FA - Boundary lines of the area of contact.

R_A, R_B, R_C, R_D, R_E, R_F - Radius at points, A,B,C,D,E and F respectively.

θ_{AB}, θ_{BC}, θ_{CD}, θ_{DE}, θ_{EF}, θ_{FA} - θ as a function of R along lines AB, BC, CD, DE, EF, and FA, respectively.

Zone 1, Zone 2, Zone 3 - Zones of the cone (Fig. 9).

dv - Infinitesimal volume

ds - Infinitesimal area

ϵ - Strain.

ϵ_{ij} - Strain components, where: i = R,θ, Z and j = R,θ,Z

e - Hydrostatic portion of the strain.

e_{ij} - Strain deviator tensor.

$\dot{\square}$ - A dot on top represents time rate, and can be applied to any variable

$\dot{\epsilon},\dot{\epsilon}_{ij}$, $\dot{e}$, $\dot{e}_{ij}$ - These are strain rate, strain-rate components, hydrostatic portion of the strain rate and strain-rate deviator tensor, respectively.

$\square_{ii}$ - Repeated index represent summation, like $\epsilon_{ii} = \epsilon_{RR} + \epsilon_{\theta\,\theta} + \epsilon_{ZZ}$.

δ_{ij} - Unit tensor called "Kronecker delta" and: equal 1 when i = j
equal 0 when i ≠ j.

σ - Stress.

σ_{ij} - Components of stress.

S - Hydrostatic portion of the stress.

S_{ij} - Components of the stress deviator.

τ - Shear stress.

γ - Shear strain.

ν - Poisson's ratio.

E - Young's modulus of elasticity.

γ - Shear angle.

δ - Displacement.

b - Strain-hardening coefficient.

ζ - Strain-rates ratio factor.

h - Feed marks height.

λ - Proportionality factor in Mises stress-strain-rate law.

I - Strain function.

J_2 - The second invariant of stress.

w - Work per unit volume.

$\dot{W}$ - Power.

$\dot{W}'$ - Weighted power.

$\dot{W}'_p$ - Partial weighted power.

$\dot{W}'_c$ - Complementary weighted power.

$\dot{W}'_{c1}$ - Complementary weighted power consumed over areas 1 and 2, respectively.

$\dot{W}_t$ - Power consumed through tangential motion.

$\dot{W}_A$ - Power consumed through feed motion.

t - Tangential force.

F_A - Feed force.

F_R - Radial force.

α, α_θ, α_R, $\Delta\alpha_R$ - Experimental values of shear angles as prescribed in Fig. 18.

THE ANALYTICAL APPROACH

A. THE PROCESS

For mathematical representation, a model spin was formulated. The geometrical relations between the cone and the roller are shown in Fig. 4. In Fig. 5 the simplified displacements field is described. This displacement field is a "geometrically admissible" field. It is also close to the actual displacements field.

The area of contact between the cone and the roller is that area where the outer surface of the cone and the roller are interfering with each other. This area takes the shape of the roller. The strain field, stress field, work, etc., were computed for the cone under the area of contact only. Although deformations exist outside of this region, they are ignored. This omission is discussed in more detail later.

As Fig. 5 indicates, the radius of any material point remains unchanged during the whole process. Radial planes in the original disc remain radial planes in the deformed cone, so for visual realization one might conceive of the original disc as being constructed from concentric thin cylinders which are slipped axially to form the final cone (see Fig. 6).

The above description does omit one crucial fact. The rings do not slip a full ring at a time. Only the portion of the ring directly affected by the roller is slipped, and as the roller advances it slips a bigger and bigger portion of the ring, until a full revolution is achieved, and the ring as a whole is displaced.

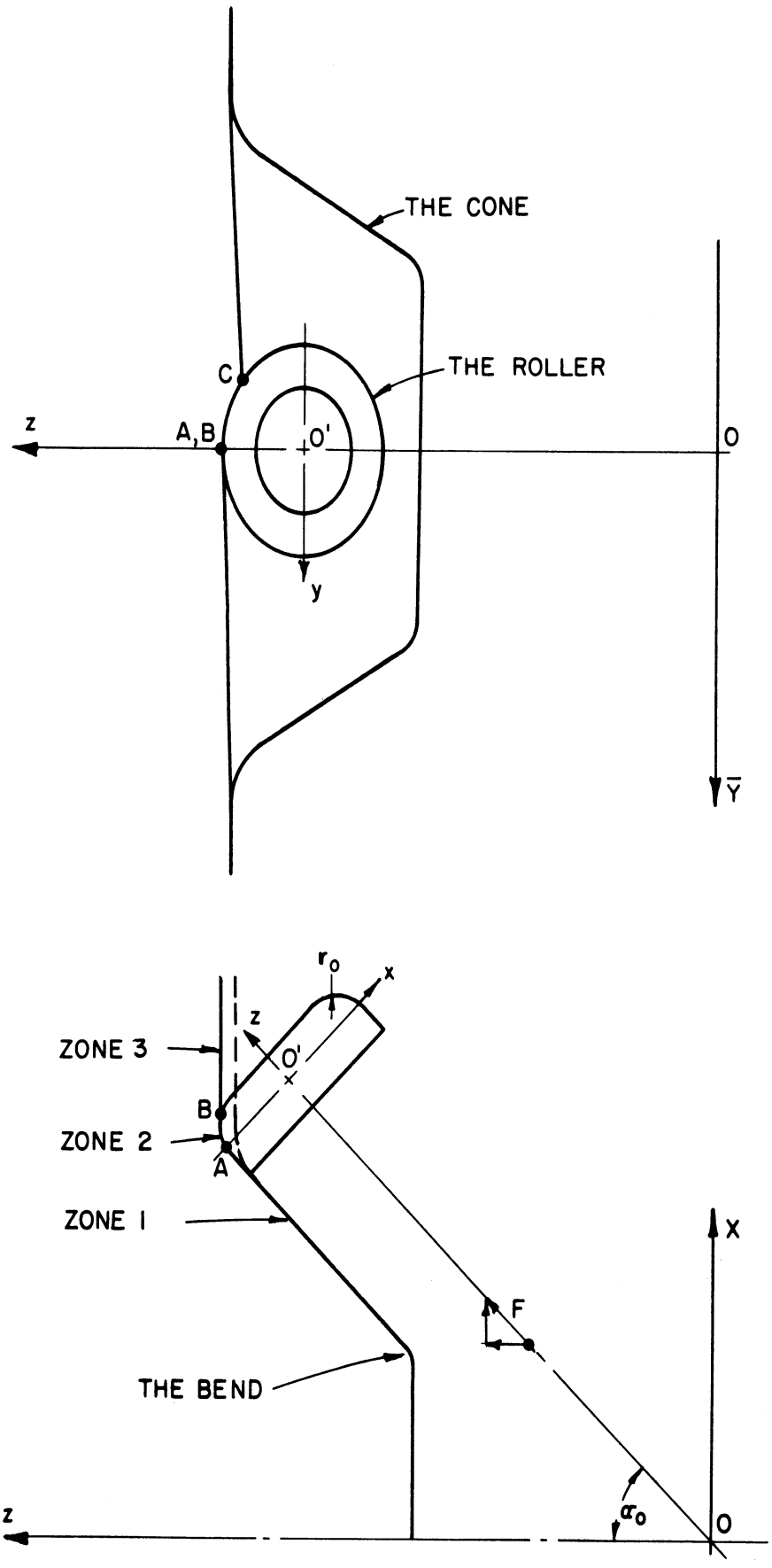

Fig. 4 - The process

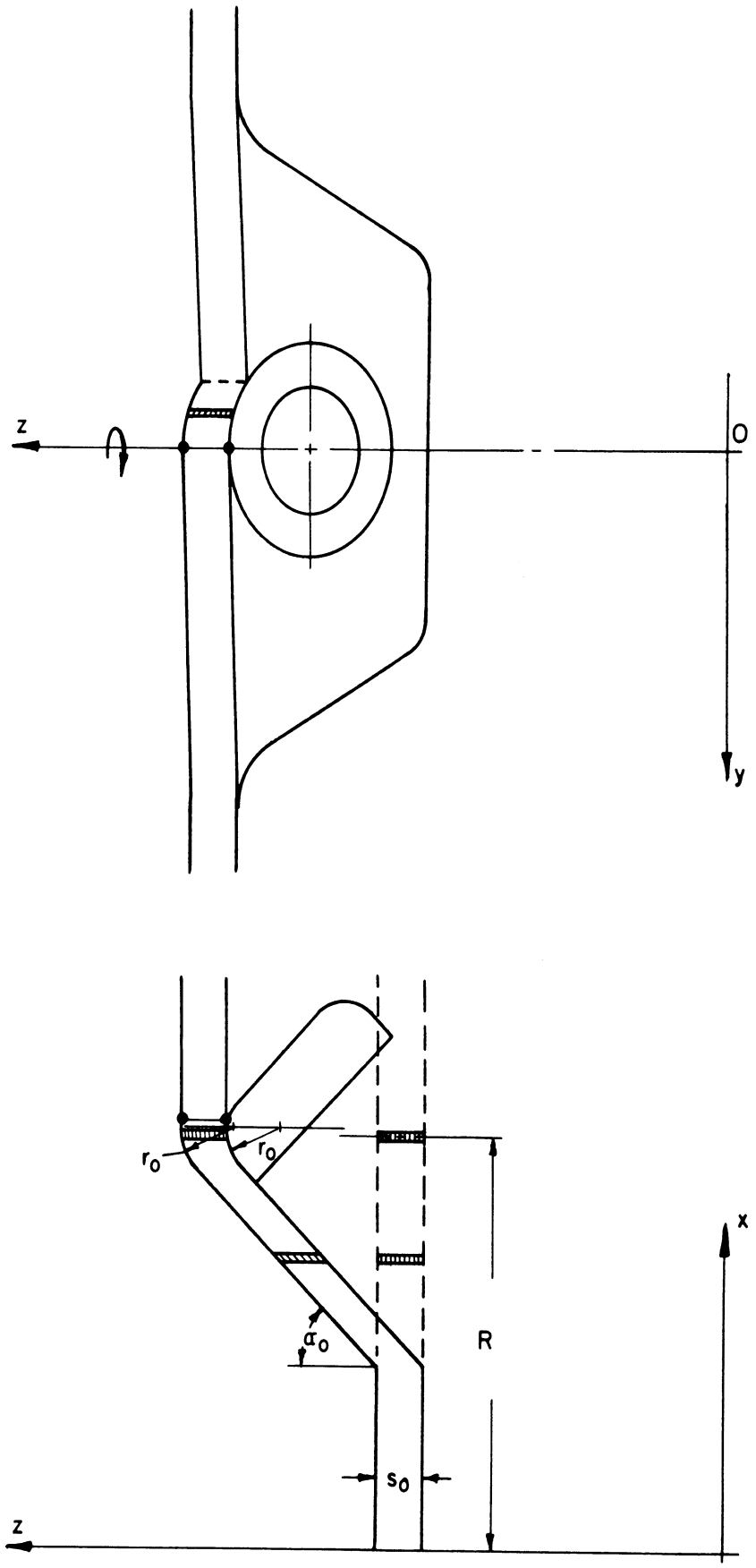

Fig. 5 - The deformations

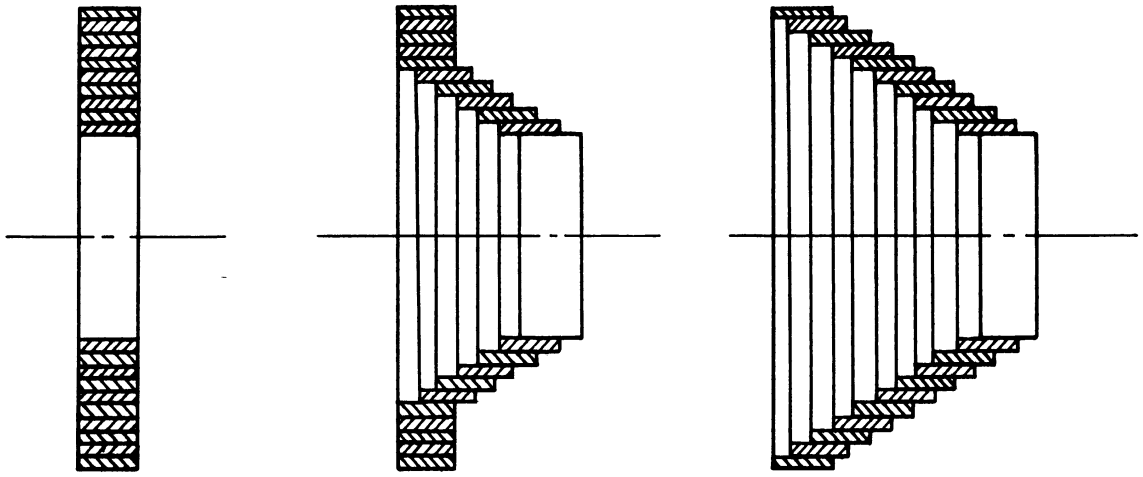

Fig. 6 – Disc analogy

Although at the completion of the deformation the cylinder is reshaped as a cylinder, during the operation the cylinders are distorted, and regain their shape only at the end. This distortion is the shear $\epsilon_{\theta z}$ and is shown in y-z plane of Fig. 5.

Fig. 7 illustrates the way a disc is displaced if it is opened to form a strip.

This model cone spinning differs in certain points from the actually spun cone. It will be more convenient to discuss these differences after describing the experimental results of the first set of experiments. The justification for choosing this model will be given later. Meanwhile, the analysis proceeds for the chosen model.

B. THE PROCESS VARIABLES

To summarize the process in terms of its independent parameters, we classify the parameters in three groups:

(1) the tool parameters,

(2) the cone parameters, and

(3) the process parameters.

The relative position of the tool toward the cone was fixed so that z axis of the tool was parallel to the side of the cone, and the tool feed is in z direction. Thus the positioning is not a variable, and is included in the standard unchanged conditions of the process.

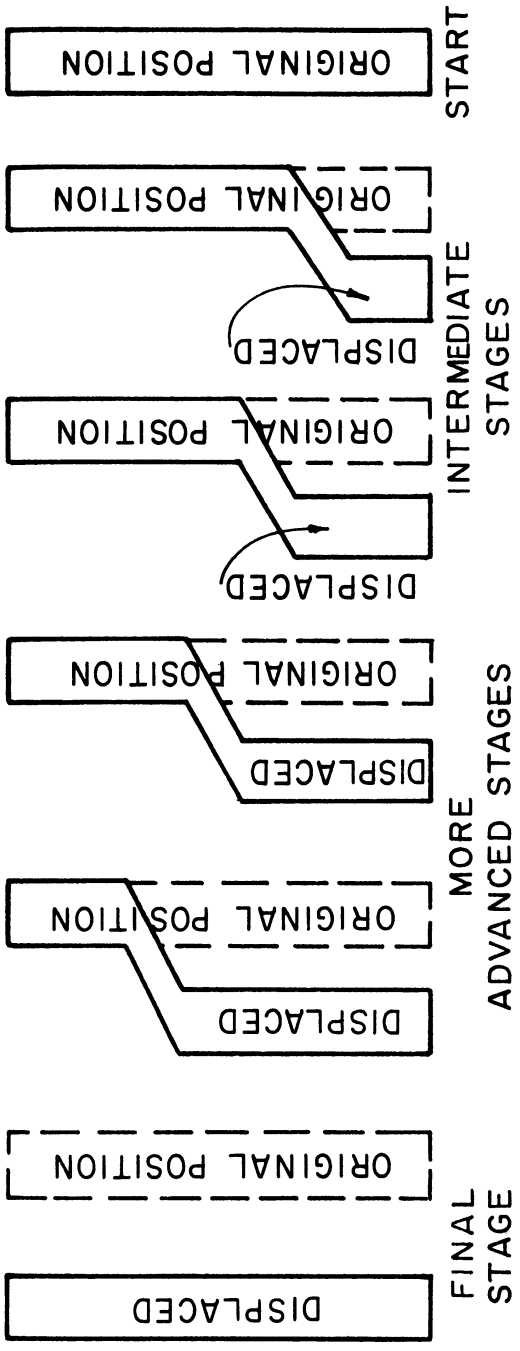

Fig. 7 - Displacing the discs

(a) The tool parameters, using only a tool of shape I in Fig. 2, are:

r_o - the roller's "round-off" radius, and

ρ_o - the roller's radius

(b) The cone parameters are:

α_o - half the included angle,

R_o - instantaneous radius at which the roller touches the cone,

R_{oMin} - cone's radius (R) at the bend,

R_{oMax} - the blank's outer radius,

S_o - the blank's thickness, and

σ_o - the cone's material yield limit at uniaxial tensial test.

(c) The process parameters are:

N - the speed in rpm, and

F - the feed in ipr.

Of these eight parameters, the cone angle ($2\alpha_o$), the cone bend radius (R_{oMin}) and outer radius (R_{oMax}), as well as the material (σ_o) and the thickness (S_o), are determined by the designer of the cone. The operation can be performed with a wide choice of the other parameters, r_o, ρ_o, N, and F. This study will enable the right choice of these last four parameters as far as the power is concerned. For a good description of the process, see part 1 of Ref. 2.

C. THE VELOCITY FIELD (U)

Let the cone be considered in the R, Θ, Z polar coordinate system. Each point of the rotating disc has rotational motion with velocity:

$$U_{\Theta} = 2\pi RN$$

around the Z axis. No change in the radius R takes place during this process, and therefore:

$$U_R = 0.$$

Layers at $0 \leq Z$ are identical with each other. The volume under the area of the instaneous contact with the roller has an additional component of the velocity (U_Z) in the z direction.

Let the velocity U_Z be computed in terms of the other two components of the velocity U_{Θ} and U_R and the geometry of the roller. Let the roller be described as the rigid body $G(R, \Theta, Z, t)=0$. In this analysis, the disc is the flowing medium, and the roller is the rigid body (see Fig. 8).

Stating that the component of the velocity of the flow, Normal to the Rigid Body, is the same for the medium as for the rigid body leads to:

$$G_R \cdot \dot{R} + G_{\Theta} \cdot \dot{\Theta} + G_Z \dot{Z} + G_t = 0$$

where

$$G_R = \frac{\partial G}{\partial R}, \quad G_{\Theta} = \frac{\partial G}{\partial \Theta}, \quad G_Z = \frac{\partial G}{\partial Z}, \quad G_t = \frac{\partial G}{\partial t}$$

$$\dot{R} = \frac{dR}{dt}, \quad \dot{\Theta} = \frac{d\Theta}{dt}, \quad \dot{Z} = \frac{dZ}{dt}$$

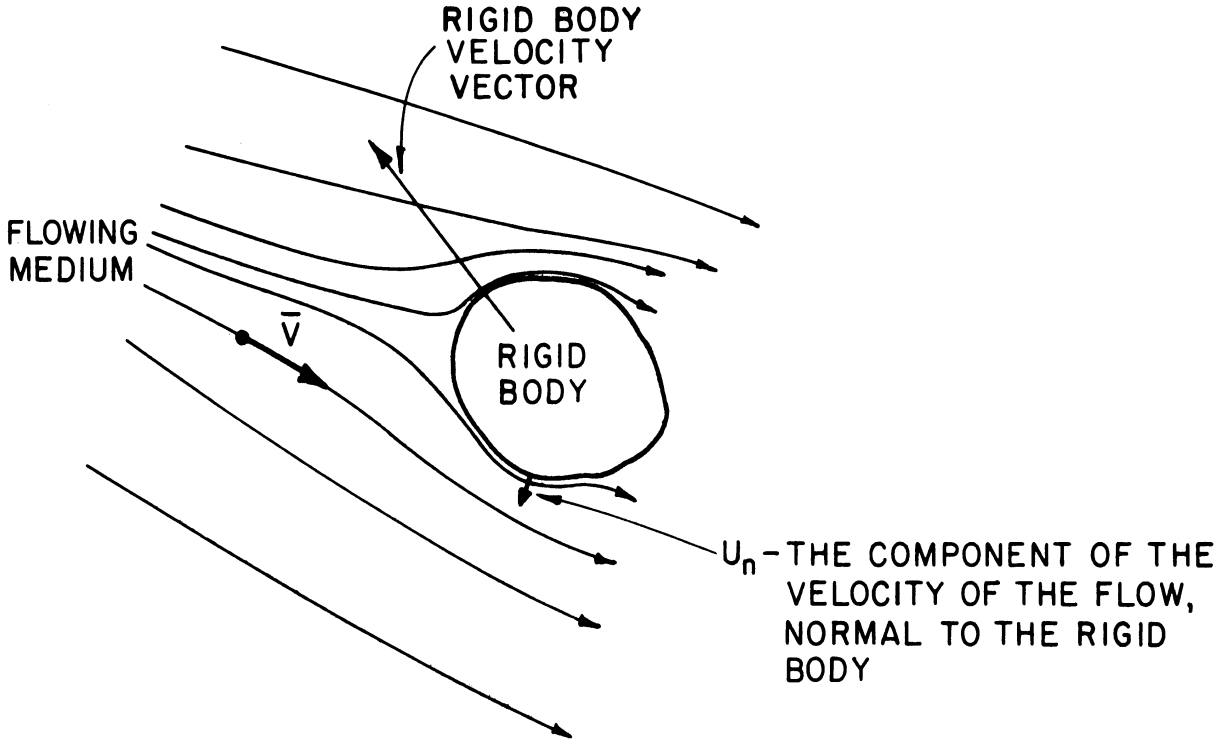

Fig. 8 - Viscous flow around an obstacle

or $$\bar{U} \cdot \Delta G = U_n = - G_t$$

where: $\bar{U}$ - the velocity vector of the medium

ΔG - the gradient of the surface of the rigid body.

$$\frac{dz}{dt} = \frac{-G_R \frac{dR}{dt} - G_\Theta \frac{d\Theta}{dt} - G_t}{G_Z} = - \frac{G_R}{G_Z} \cdot \frac{dR}{dt} - \frac{G_\Theta}{G_Z} \cdot \frac{d\Theta}{dt} - \frac{G_t}{G_Z}$$

Knowing the values $\frac{dR}{dt} = U_R = 0$ and $\frac{d\Theta}{dt} = \frac{U_\Theta}{R} = 2\pi N$,

one gets: $$\frac{dZ}{dt} = U_z = 2\pi N \frac{\partial Z}{\partial \Theta} + \frac{\partial Z}{\partial t}$$

Evaluating the number of revolutions from time $t = t_o$, one gets:

$$n = N \cdot (t - t_o)$$

and deriving with respect to t,

$$\frac{dn}{dt} = N$$

and thus one continues and gets

$$\frac{dz}{dt} = U_z = 2\pi N \frac{\partial z}{\partial \Theta} + \frac{\partial z}{\partial n} \cdot \frac{dn}{dt} = 2\pi N \frac{\partial z}{\partial \Theta} + N \frac{dz}{\partial n} = N \cdot \left[2\pi \frac{\partial z}{\partial \Theta} + \frac{\partial Z}{\partial n} \right]$$

Another approach, using Euler's method (the observer is stationary) follows. If the rigid body equation is

$$F(R, \Theta, Z, n) = 0$$

it gives z as a function of R, θ and n.

$$z = H(R, \theta, n)$$

$$n = f(t) = N(t-t_o)$$

$$dz = \frac{\partial z}{\partial R} dR + \frac{\partial z}{\partial \theta} d\theta + \frac{\partial z}{\partial n} dn$$

$$U_z = \frac{dz}{dt} = \frac{\partial z}{\partial R}\frac{dR}{dt} + \frac{\partial z}{\partial \theta}\frac{d\theta}{dt} + \frac{\partial z}{\partial n}\frac{dn}{dt}$$

inserting the values $\frac{dR}{dt} = U_R = 0$, $\frac{d\theta}{dt} = \frac{U_\theta}{R} = 2\pi N$, and $\frac{dn}{dt} = N$, one gets

the same expression for U_z as before.

$$U_z = N\left[2\pi \frac{\partial z}{\partial \theta} + \frac{\partial z}{\partial n}\right]$$

Summing up the velocity field under direct effect of the roller, one gets:

$$\left.\begin{aligned} U_R &= 0 \\ U_\theta &= 2\pi RN \\ U_z &= N\left[2\pi \frac{\partial z}{\partial \theta} + \frac{\partial z}{\partial n}\right] \end{aligned}\right\} \qquad (1)$$

where the derivatives $\frac{\partial z}{\partial \theta}$ and $\frac{\partial z}{\partial n}$ are yet to be defined from the geometry

of the roller.

D. THE STRAIN-RATES FIELD

The rates of deformation[3] in cylindrical polar coordinates assume

the form:

$$\dot{\epsilon}_{RR} = \frac{\partial U_R}{\partial R}, \quad \dot{\epsilon}_{\theta\theta} = \frac{U_R}{R} + \frac{1}{R} \cdot \frac{\partial U_\theta}{\partial \theta}; \quad \dot{\epsilon}_{zz} = \frac{\partial U_z}{\partial Z}$$

$$\dot{\epsilon}_{R\theta} = \tfrac{1}{2}\left(\frac{1}{R}\,\frac{\partial U_R}{\partial \theta} + \frac{\partial U_\theta}{\partial R} - \frac{U_\theta}{R}\right)$$

$$\dot{\epsilon}_{RZ} = \tfrac{1}{2}\left(\frac{\partial U_R}{\partial Z} + \frac{\partial U_Z}{\partial R}\right)$$

$$\dot{\epsilon}_{\theta Z} = \tfrac{1}{2}\left(\frac{\partial U_\theta}{\partial Z} + \frac{\partial U_Z}{R\partial \theta}\right)$$

This description is of the general case where the "Euler Method" is used, which means that the observer is stationary. In the specific case of the velocity field of Eqs. (1), where

$$U_R = 0$$

and

$$U_\theta = 2\pi RN,$$

one can develop the strain-rates field further. Because layers at $0 \leq Z \leq S_o$ are identical with each other, we can infer that no variable is dependent on z direction. And therefore

$$\dot{\epsilon}_{zz} = \frac{\partial U_z}{\partial Z} = 0$$

and also

$$\frac{\partial U_R}{\partial Z} = \frac{\partial U_\theta}{\partial Z} = 0$$

Because

$$U_R = 0,$$

$$\dot{\epsilon}_{RR} = \frac{\partial U_R}{\partial R} = 0$$

$$\dot{\epsilon}_{\theta\theta} = \frac{U_R}{R} + \frac{1}{R}\frac{\partial U_\theta}{\partial \theta} = \frac{0}{R} + \frac{1}{R}\frac{\partial}{\partial \theta}(2\pi RN) \equiv 0$$

$$\dot{\epsilon}_{R\theta} = \tfrac{1}{2}\left(\frac{1}{R}\frac{\partial U_R}{\partial \theta} + \frac{\partial U_\theta}{\partial R} - \frac{U_\theta}{R}\right) = \tfrac{1}{2}\left(\frac{\partial}{\partial R}(2\pi RN) - \frac{2\pi RN}{R}\right) = \tfrac{1}{2}(2\pi N - 2\pi N) = 0$$

$$\dot{\epsilon}_{RZ} = \tfrac{1}{2}\left(\frac{\partial U_R}{\partial Z} + \frac{\partial U_Z}{\partial R}\right) = \tfrac{1}{2}\frac{\partial U_Z}{\partial R}$$

$$\dot{\epsilon}_{\theta Z} = \tfrac{1}{2}\left(\frac{\partial U_\theta}{\partial Z} + \frac{\partial U_Z}{R\partial \theta}\right) = \frac{1}{2R}\frac{\partial U_Z}{\partial \theta}$$

And thus the strain-rates field is given in the form

$$\left.\begin{aligned} \dot{\epsilon}_{RZ} &= \frac{1}{2}\frac{\partial U_Z}{\partial R} \\ \dot{\epsilon}_{\theta Z} &= \frac{1}{2R}\frac{\partial U_Z}{\partial \theta} \\ \text{All other } \dot{\epsilon}_{ij} &= 0 \end{aligned}\right\} \qquad (2)$$

E. THE STATE OF STRESS

The Levy-Mises stress-plastic-strain-rate law, with the use of stress deviators and strain deviators, is written:

$$\dot{e}_{ij} = \lambda S_{ij} \qquad (3)$$

where S_{ij} is the stress deviator tensor,

$\dot{e}_{ij}$ is the plastic-strain-rate deviator tensor, and

λ is the proportionality factor, and is a function of the strain rates.

From the assumption that there is no plastic volumetric change, it follows that the plastic-strain-rate deviator is equal to the plastic strain rate itself.

$$\dot{e} = \frac{1}{3}\dot{e}_{ii}$$

where e is the hydrostatic strain,

$\dot{e}$ is the hydrostatic strain rate, and

$\dot{e}_{ii} = \dot{e}_{11} + \dot{e}_{22} + \dot{e}_{33} = 0$ (volume constancy);

$\therefore \dot{e} = \frac{1}{3}\dot{e}_{ii} = 0$, and

$\therefore \dot{\epsilon}_{ij} = \dot{e}_{ij} + \dot{e}\delta_{ij} = \dot{e}_{ij}$

where $\dot{\epsilon}_{ij}$ is the plastic-strain-rate tensor. Because "Mises Material" has no elastic strains, it follows that the plastic strains are the only existing ones. The stress-strain-rate relations become:

$$\dot{\epsilon}_{ij} = \mu S_{ij} \tag{4}$$

Let a term I be defined such that

$$I = \frac{1}{2}\dot{\epsilon}_{ij}\dot{\epsilon}_{ij} \tag{5}$$

Substituting (4) in (5), it follows that

$$I = \frac{1}{2}\dot{\epsilon}_{ij}\dot{\epsilon}_{ij} = \mu^2 \frac{1}{2} S_{ij}S_{ij}$$

Substituting "Mises Yield Condition"

$J_2 = \frac{1}{2} S_{ij}S_{ij} = k^2$ in the preceding equation, one gets:

$$I = \mu^2 k^2$$

$$\mu = \pm \frac{\sqrt{I}}{k}$$

and Mises "stress-strain-rate" law becomes

$$\left.\begin{aligned} \dot{\epsilon}_{ij} &= \pm \frac{\sqrt{I}}{k} S_{ij} = \pm \frac{\sqrt{\frac{1}{2}\cdot\dot{\epsilon}_{kl}\cdot\dot{\epsilon}_{kl}}}{k} S_{ij} \\ \text{or:}\quad S_{ij} &= \pm \frac{k\ \dot{\epsilon}_{ij}}{\sqrt{\frac{1}{2}\cdot\dot{\epsilon}_{kl}\cdot\dot{\epsilon}_{kl}}} \end{aligned}\right\} \quad (6)$$

The stress deviator field is therefore:

$$\left.\begin{aligned} G_{RZ} = S_{RZ} &= \pm \frac{k\ \dot{\epsilon}_{RZ}}{\sqrt{\dot{\epsilon}^2_{Rz} + \dot{\epsilon}^2_{\Theta Z}}} \\ G_{\Theta Z} = S_{\Theta Z} &= \pm \frac{k\ \dot{\epsilon}_{\Theta Z}}{\sqrt{\dot{\epsilon}^2_{RZ} + \dot{\epsilon}^2_{\Theta z}}} \\ \text{All other } S_{ij} &= 0 \end{aligned}\right\} \quad (7)$$

The sign is to be chosen from physical considerations. Whether it is plus or minus is not relevant in this study.

F. THE POWER

Let the rate of work per unit volume be

$$\dot{w} = \sigma_{ij}\ \dot{\epsilon}_{ij} \quad (8)$$

The stress tensor can be separated into stress deviator and hydrostatic stress.

$$\dot{w} = \sigma_{ij}\dot{\epsilon}_{ij} = (S_{ij} + S\delta_{ij})\dot{\epsilon}_{ij} = S_{ij}\dot{\epsilon}_{ij} + S\dot{\epsilon}_{ij}\delta_{ij} = S_{ij}\dot{\epsilon}_{ij} + S\dot{\epsilon}_{ii}$$

where: S - the hydrostatic stress $S = \frac{1}{3}\sigma_{ii}$

And because of the incompressibility,

$$\dot{\epsilon}_{ii} = 0;$$

$$\dot{w} = S_{ij}\dot{\epsilon}_{ij} \qquad (9)$$

Substituting for $\dot{\epsilon}_{ij}$ its value from Eq. (6), one gets

$$\dot{w} = \pm S_{ij}S_{ij}\frac{\sqrt{\frac{1}{2}\dot{\epsilon}_{kl}\dot{\epsilon}_{kl}}}{k}$$

Substituting now the yield condition, $J_2 = \frac{1}{2}S_{ij}S_{ij} = k^2$, one gets:

$$\dot{w} = \pm \frac{2k^2}{k}\sqrt{\frac{1}{2}\dot{\epsilon}_{kl}\dot{\epsilon}_{kl}} = \pm 2k\sqrt{\frac{1}{2}\dot{\epsilon}_{ij}\dot{\epsilon}_{ij}}$$

It is now desired to replace k by the yield at uniaxial tensile test.

For uniaxial stress:

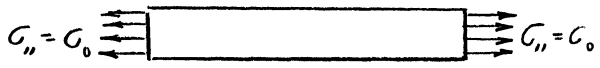

$$S = \frac{1}{3}\sigma_0 \quad S_1 = \frac{2}{3}\sigma_0 \quad S_2 = S_3 = -\frac{1}{3}\sigma_0$$

All other $S_{ij} = 0$

Mises Yield condition gives

$$J_2 = \frac{1}{2}S_{ij}S_{ij} = \frac{1}{2}\left(\frac{4}{9} + \frac{1}{9} + \frac{1}{9}\right)\sigma_0^2 = \frac{1}{3}\sigma_0^2 = k^2$$

$$k = \frac{\sigma_0}{\sqrt{3}}$$

It follows that the rate of work per unit volume is:

$$\dot{w} = \pm \frac{2}{\sqrt{3}} \sigma_o \sqrt{\frac{1}{2} \dot{\epsilon}_{ij} \dot{\epsilon}_{ij}} \qquad (10)$$

Defining work done on a system to be positive, it follows that:

$$\dot{w} = \frac{2}{\sqrt{3}} \sigma_o \sqrt{\frac{1}{2} \dot{\epsilon}_{ij} \dot{\epsilon}_{ij}}$$

With the particular strain-rate field in this case,

$$\dot{w} = \frac{2}{\sqrt{3}} \sigma_o \sqrt{\dot{\epsilon}_{RZ}^2 + \dot{\epsilon}_{\theta Z}^2} = \frac{2}{\sqrt{3}} \sigma_o \sqrt{\left(\frac{1}{2} \cdot \frac{\partial U_z}{\partial R}\right)^2 + \left(\frac{1}{2R} \frac{\partial U_z}{\partial \theta}\right)^2}$$

$$\dot{w} = \frac{\sigma_o}{\sqrt{3}} \sqrt{\left(\frac{\partial U_z}{\partial R}\right)^2 + \left(\frac{1}{R} \cdot \frac{\partial U_z}{\partial \theta}\right)^2}$$

The rate of work for the deformed cone is

$$\dot{W} = \int_{\text{volume}} \frac{\sigma_o}{\sqrt{3}} \sqrt{\left(\frac{\partial U_z}{\partial R}\right)^2 + \left(\frac{1}{R} \cdot \frac{\partial U_z}{\partial \theta}\right)^2} \, dV = \frac{\sigma_o}{\sqrt{3}} \int_{\text{Surface}} \left[\int_{z=0}^{S_o} \sqrt{\left(\frac{\partial U_z}{\partial R}\right)^2 + \left(\frac{1}{R} \frac{\partial U_z}{\partial \theta}\right)^2} \, dz \right] ds$$

Because the strains are independent on z direction, one can first integrate with respect to z and get:

$$\dot{W} = \frac{\sigma_o S_o}{\sqrt{3}} \int_{\text{surface}} \sqrt{\left(\frac{\partial U_z}{\partial R}\right)^2 + \left(\frac{1}{R} \cdot \frac{\partial U_z}{\partial \theta}\right)^2} \, ds$$

$$\dot{W} = \frac{G_o S_o}{\sqrt{3}} \int_{\theta} \int_{R} R \sqrt{\left(\frac{\partial U_z}{\partial R}\right)^2 + \left(\frac{1}{R} \cdot \frac{\partial U_z}{\partial \theta}\right)^2} \, dR d\theta \qquad (11)$$

MATHEMATICAL DESCRIPTION OF THE PROCESS

A. THE SETS OF AXIS AND THEIR TRANSFORMATION

Consider three coordinate systems:

(1) (x,y,z) cartesian coordinate system, with the origin O'. The axis z is the axis of cylindrical symmetry for the roller, and the origin is the center of the torical portion of the roller.

(2) (X,Y,Z) cartesian coordinate system, with the origin O. The axis Z is the axis of cylindrical symmetry for the cone.

(3) (R,θ,Z) cylindrical polar coordinates with the same origin O and Z axis as the second cartesian system.

The directional cosines for transformation from (x,y,z) system to (X,Y,Z) system and vice versa can be represented in the following way.

Table I - Directional Cosines

	x	y	z
X	$\cos \alpha_o$	0	$\sin \alpha_o$
Y	0	1	0
Z	$-\sin\alpha_o$	0	$\cos\alpha_o$

The transformation scheme is according to the following equation.

$$\left.\begin{aligned} x_i &= a_i + a_{ij}X_j \\ X_j &= b_j + a_{ji}x_i \end{aligned}\right\} \qquad (12)$$

where: i = 1,2,3 denote the column number in Table I,

j = 1,2,3 denote the raw number in Table I,

a_i = denote the coordinates of the origin 0 in the (x,y,z) coordinates system,

$a_1 = a_2 = 0$

$a_3 = -Fn$,

b_j = denote the coordinates of the origin 0' in the (X,Y,Z) coordinate system,

$b_1 = Fn \sin \alpha_o$,

$b_2 = 0$,

$b_3 = Fn \cos \alpha_o$,

$x_1 = x$,

$x_2 = y$,

$x_3 = x$,

$X_1 = X$,

$X_2 = Y$, and

$X_3 = Z$.

The transformation is now getting this shape:

$$x_1 = x = a_1 + a_{11}X_1 + a_{12}X_2 + a_{13}X_3 = a_{11}X_1 + a_{13}X_3 = X \cos \alpha_o - Z \sin \alpha_o$$

$$x_2 = y = a_2 + a_{21}X_1 + a_{22}X_2 + a_{23}X_3 = a_{22}X_2 = Y$$

$$x_3 = z = a_3 + a_{31}X_1 + a_{32}X_2 + a_{33}X_3 = a_3 + a_{31}X_1 + a_{33}X_3 = -Fn + X\sin \alpha_o + Z\cos \alpha_o$$

And applying the second of Eqs. (12), one gets:

$$X_1 = X = x \cos \alpha_o + z \sin \alpha_o + Fn \sin \alpha_o$$

$$X_2 = Y = y$$

$$X_3 = Z = - x \sin \alpha_o + z \cos \alpha_o + Fn \cos \alpha_o$$

The transformation from R, Θ, Z system to (X,Y,Z) system is to be performed by:

$$X = R \cos \Theta$$

$$Y = R \sin \Theta$$

$$Z = Z$$

and from (X,Y,Z) to (R,Θ,Z) is performed through

$$R = \sqrt{X^2 + Y^2}$$

$$\Theta = \cos^{-1} \frac{X}{\sqrt{X^2+Y^2}} = \sin^{-1} \frac{Y}{\sqrt{X^2+Y^2}} = \tan^{-1} \frac{Y}{X}$$

$$Z = Z$$

The transformation from either system to any other system of the three is now given.

$$\begin{cases} \begin{cases} x = X \cos \alpha_o - Z \sin \alpha_o = R \cos \Theta \cos \alpha_o - Z \sin \alpha_o \\ y = Y = R \sin \Theta \\ z = X \sin \alpha_o + Z \cos \alpha_o - Fn = R \cos \Theta \sin \alpha_o + Z \cos \alpha_o - Fn \end{cases} \\ \begin{cases} X = R \cos \Theta = x \cos \alpha_o + z \sin \alpha_o + Fn \sin \alpha_o \\ Y = R \sin \Theta = y \\ Z = Z = -x \sin \alpha_o + z \cos \alpha_o + Fn \cos \alpha_o \end{cases} \\ \begin{cases} R = \sqrt{X^2 + Y^2} = \sqrt{(x \cos \alpha_o + z \cos \alpha_o + Fn \sin \alpha_o)^2 + y^2} \\ \Theta = \cos^{-1} \frac{X}{\sqrt{X^2+Y^2}} = \sin^{-1} \frac{Y}{\sqrt{X^2+Y^2}} = \cos^{-1} \frac{x \cos \alpha_o + z \sin \alpha_o + Fn \sin \alpha}{\sqrt{(x \cos \alpha_o + z \sin \alpha_o + Fn \sin \alpha_o)^2 + y}} \\ Z = z = -x \sin \alpha_o + z \cos \alpha_o + Fn \cos \alpha_o \end{cases} \end{cases} \tag{13}$$

B. THE ROLLER

The roller is composed of a half torus and a cylinder.

The half torus exists for $z \geq 0$. Its equations are:

$$\left[\sqrt{x^2 + y^2} - \rho_o\right]^2 + z^2 - r_o^2 = 0 \tag{14}$$

$$G = \left[\sqrt{(R\cos\theta\cos\alpha_o - Z\sin\alpha_o)^2 + R^2\sin^2\theta} - \rho_o\right]^2$$
$$+\left[R\cos\theta\sin\alpha_o + Z\cos\alpha_o - Fn\right]^2 - r_o^2 = 0 \qquad (14)$$

Let the second of Eqs. (14) be referred to as $G = 0$, or $G(R,\theta,Z) = 0$.

The cylindrical portion of the roller exists only for $z \leq 0$. Its equation is:

$$x^2 + y^2 - (r_o + \rho_o)^2 = 0$$

By transforming this equation to (R,θ,Z) axis, one gets:

$$(R\cos\theta\cos\alpha_o - Z\sin\alpha_o)^2 + R^2\sin^2\theta - (r_o + \rho_o)^2 = 0$$

$$R\cos\theta\cos\alpha_o - Z\sin\alpha_o = \pm\sqrt{(\rho_o + r_o)^2 - R^2\sin^2\theta}$$

$$Z = \frac{1}{\sin\alpha_o}\left[R\cos\theta\cos\alpha_o \pm \sqrt{(\rho_o + r_o)^2 - R^2\sin^2\theta}\right]$$

From geometrical considerations, the plus sign is to be chosen for that portion of the roller that is in touch with the cone. The equation of the cylindrical portion of the roller becomes

$$\left.\begin{aligned} &x^2 + y^2 - (r_o + \rho_o)^2 = 0 \\ &Z = \frac{1}{\sin\alpha_o}\left[R\cos\theta\cos\alpha_o + \sqrt{(\rho_o + r_o)^2 - R^2\sin^2\theta}\right] \end{aligned}\right\} \qquad (15)$$

C. THE CONE

Let the cone be separated into three zones. Zone 1 is the already deformed portion of the cone. This zone is bounded by the bend on one end and by the cylinder of the same radius as spiral A is leaving. Spiral A is the trace that point A on the roller leaves on the cone. Zone 2 is the zone

being deformed; it is bounded by the speralic areas of radius as that of spiral A and as that of spiral B. Spiral B is the trace that point B on the roller leaves on the cone. Zone 3 is the yet undeformed disc from spiral B and up.

$$\left.\begin{aligned}
&\underline{\text{Spiral A:}}\quad R_A = F\left(n - \frac{\theta}{2\pi}\right)\sin\alpha_o - (r_o + \rho_o)\cos\alpha_o \\
&\qquad\qquad Z_A = F\left(n - \frac{\theta}{2\pi}\right)\cos\alpha_o + (r_o + \rho_o)\sin\alpha_o \\
&\underline{\text{Spiral B:}}\quad R_B = F\left(n - \frac{\theta}{2\pi}\right)\sin\alpha_o - \rho_o\cos\alpha_o \\
&\qquad\qquad Z_B = F\left(n - \frac{\theta}{2\pi}\right)\cos\alpha_o + \rho_o\sin\alpha_o
\end{aligned}\right\} \qquad (16)$$

Zone 2 of the Cone

The generating circle AB of the torus is:

$$\left\{\begin{aligned}
&(x + \rho_o)^2 + z^2 = r_o^2 \\
&y = 0 \qquad\qquad (17)\\
&(R\cos\alpha_o - Z\sin\alpha_o + \rho_o)^2 + (R\sin\alpha_o + Z\cos\alpha_o - Fn)^2 - r_o^2 = 0 \\
&\theta = 0
\end{aligned}\right.$$

or:

And thus, zone 2 is:

$$(R\cos\alpha_o - Z\sin\alpha_o + \rho_o)^2 + \left[R\sin\alpha_o + Z\cos\alpha_o - F\left(n - \frac{\theta}{2\pi}\right)\right]^2 - r_o^2 = 0$$

Because the zone of interest is at the contact area between the cone and the roller, for which $\theta \simeq 2\pi$, one can approximate $\frac{\theta}{2\pi}$ by 1. Thus, the approximate equation of the cone at the area of contact is:

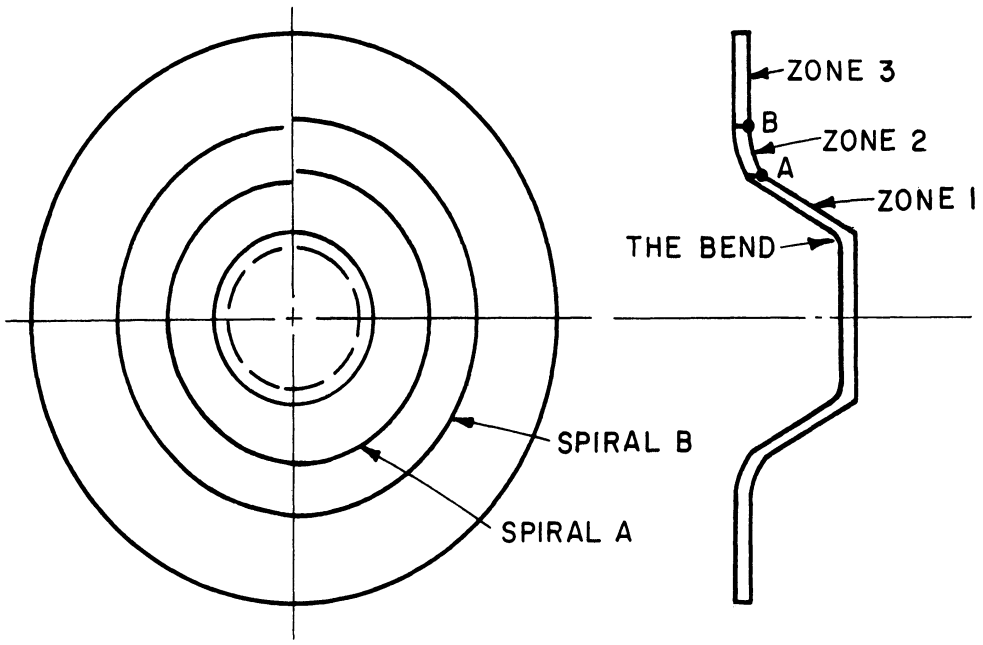

Fig. 9-The cones' zones

Area A: (3+4+5+6)

$$G = \left[\sqrt{(R\cos\theta\cos\alpha_0 - Z\sin\alpha_0)^2 + R^2\sin^2\Theta} - \rho_0\right]^2 +$$

$$+ \left[R\cos\theta\sin\alpha_0 + Z\cos\alpha_0 - Fn\right]^2 - r_0^2 = 0$$

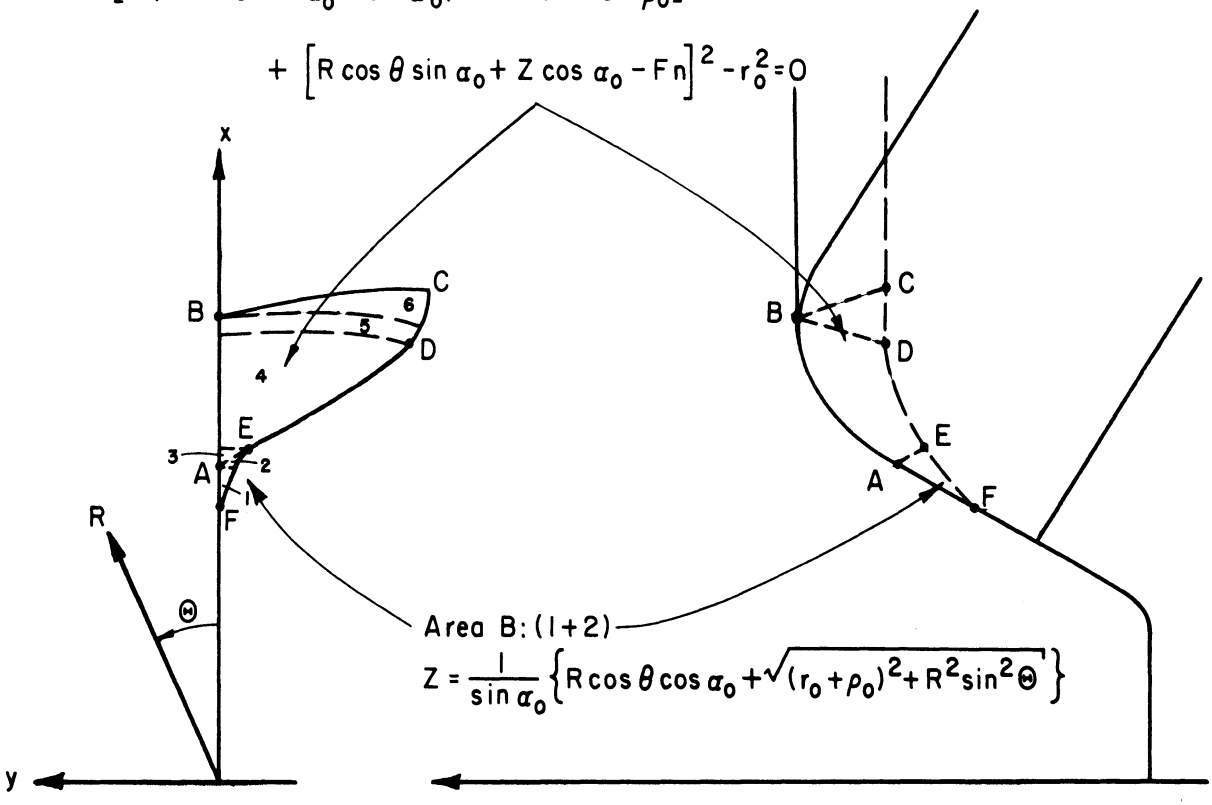

Fig. 10- The area of contact

$$(R\cos\alpha_o - Z\sin\alpha_o + \rho_o)^2 + [R\sin\alpha_o + Z\cos\alpha_o - F(n\text{-}1)]^2 - r_o^2 = 0$$

$$Z^2 - 2Z\underbrace{[\sin\alpha_o\,(R\cos\alpha_o + \rho_o) - \cos\alpha_o\,[R\sin\alpha_o - F(n\text{-}1)]]}_{b}$$

$$+\underbrace{(R\cos\alpha_o + \rho_o)^2 + [R\sin\alpha_o - F(n\text{-}1)]^2 - r_o^2}_{c} = 0$$

$$Z_{1,2} = b \pm \sqrt{b^2 - c}$$

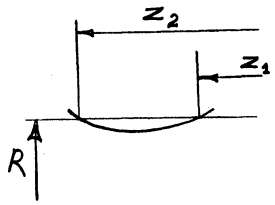

For the area of contact $Z = Z_2$

$$Z = b + \sqrt{b^2 - c}$$

where: $b = \rho_o \sin\alpha_o + F(n\text{-}1)\cos\alpha_o$ (18)

$$c = (R\cos\alpha_o + \rho_o)^2 + [R\sin\alpha_o - F(n\text{-}1)]^2 - r_o^2$$

Zone 3 of the Cone

For Zone 3 of the cone:

$$Z = F\left(n - \frac{\theta}{2\pi}\right)\cos\alpha_o + \rho_o\sin\alpha_o + r_o \simeq F(n\text{-}1)\cos\alpha_o + \rho_o\sin\alpha_o + r_o \quad (19)$$

D. THE AREA OF CONTACT

The area of contact between the roller and the cone takes the shape of the roller.

Let the area of contact be composed of two main areas. Area A will be that shaped like the torus, and Area B will be that shaped cylindrically (see Fig. 10). Let the boundary ABCDEFA be defined line by line.

Line AB is the circle described by Eqs. (17).

Line BC The contour of line BC can be found by deriving $\frac{\partial Z}{\partial R} = 0$

on the equation of the torus G = 0. However, because the determination of this line gets involved, it can be approximated by a circle passing through point B around the main axis of the torus (see Fig. 11).

The plane of the circle can be described by:

$$z = r_o \cos \alpha_o$$

And the circle $x^2 + y^2 = (\rho_o + r_o \sin \alpha_o)^2$

In the (R,θ,Z) axis, line BC will become:

$$\begin{cases} R \cos \theta \sin \alpha_o + Z \cos \alpha_o - Fn - r_o \cos \alpha_o = 0 \\ (R \cos \theta \cos \alpha_o - Z \sin \alpha_o)^2 + R^2 \sin^2 \theta - (\rho_o + r_o \sin \alpha_o)^2 = 0 \end{cases}$$

Inserting $Z = \frac{1}{\cos \alpha_o} (Fn + r_o \cos \alpha_o - R \cos \theta \sin \alpha_o)$ from the first equation into the second equation, one gets

$$\left[R \cos \theta \cos \alpha_o - (Fn + r_o \cos \alpha_o - R \cos \theta \sin \alpha_o) \tan \alpha_o\right]^2 + R^2 \sin^2 \theta - (\rho_o + r_o \sin \alpha_o)^2 = 0$$

This equation of line BC is written implicitly with respect to R and θ.

Line CD For Line CD the torus G = 0 cuts Zone 3 of the cone Eq. (19). Repeating the equations once more, one gets:

$$G = \left[\sqrt{(R \cos \theta \cos \alpha_o - Z \sin \alpha_o)^2 + R^2 \sin^2 \theta} - \rho_o\right]^2 + \left[R \cos \theta \sin \alpha_o + Z \cos \alpha_o - Fn\right]^2 - r_o^2 = 0$$

where: $Z = F(n-1) \cos \alpha_o + \rho_o \operatorname{Sin} \alpha_o + r_o^2$

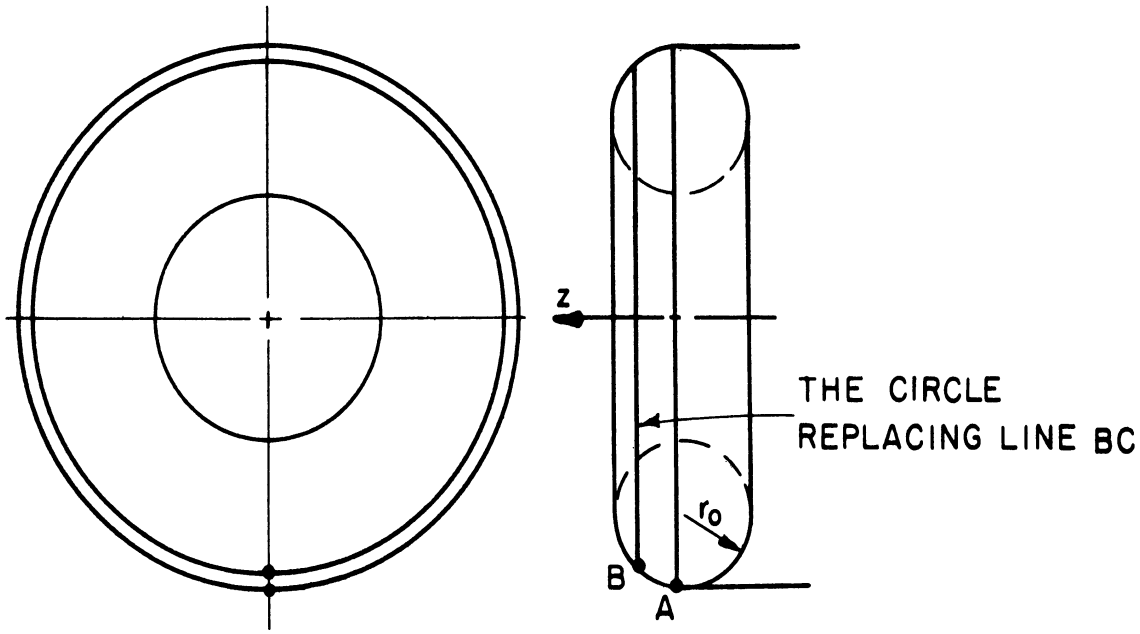

Fig. 11 - Line BC

Line DE At line DE, the torus cuts Zone 2 of the cone:

$$G = \left[\sqrt{(R\cos\theta\cos\alpha_o - Z\sin\alpha_o)^2 + R^2\sin^2\theta} - \rho_o\right]^2 + \left[R\cos\theta\sin\alpha_o + Z\cos\alpha_o - Fn\right]^2 - r_o^2 = 0$$

where: $Z = b + \sqrt{b^2 - c}$

$$b = \rho_o\sin\alpha_o + F(n-1)\cos\alpha_o$$

$$c = (R\cos\alpha_o + \rho_o)^2 + \left[R\sin\alpha_o - F(n-1)\right]^2 - r_o^2$$

Line EA is on the plane $z = 0$

From the transformation scheme (Eq. 13)

$$z = R\cos\theta\sin\alpha_o + Z\cos\alpha_o - Fn = 0$$

$$\therefore \cos\theta = \frac{Fn - Z\cos\alpha_o}{R\sin\alpha_o}$$

Substituting the right hand of the preceding equation for $\cos\theta$ in the equation of the cylinder,

$$(R\cos\theta\cos\alpha_o - Z\sin\alpha_o)^2 + R^2\sin^2\theta - (r_o + \rho_o)^2 = 0$$

one gets:

$$\left[(Fn - Z\cos\alpha_o)\cot\alpha_o - Z\sin\alpha_o\right]^2 + R^2\left[1 - \left(\frac{Fn - Z\cos\alpha_o}{R\sin\alpha_o}\right)^2\right] = (r_o + \rho_o)^2$$

$$\left[(Fn - Z\cos\alpha_o)\cot\alpha_o - Z\sin\alpha_o\right]^2 - \left(\frac{Fn - z\cos\alpha_o}{\sin\alpha_o}\right)^2 = (\rho_o + r_o)^2 - R^2$$

$$\left[Fn\cot\alpha_o - Z(\cos\alpha_o\cdot\cot\alpha_o + \sin\alpha_o)\right]^2\cdot\sin^2\alpha_o - (Fn - Z\cos\alpha_o)^2 = \left[(\rho_o + r_o)^2 - R^2\right]\cdot\sin^2\alpha_o$$

$$\left[Fn \cos \alpha_o - Z(\cos^2 \alpha_o + \sin^2 \alpha_o)\right]^2 - (Fn - Z \cos \alpha_o)^2$$
$$= \left[(\rho_o + r_o)^2 - R^2 \right] \cdot \sin^2 \alpha_o$$

$$(Fn \cos \alpha_o - Z)^2 - (Fn - Z \cos \alpha_o)^2 = \left[(\rho_o + r_o)^2 - R^2\right] \sin^2 \alpha_o$$

$$(Fn)^2(\cos^2 \alpha_o - 1) - 2Z (\cos \alpha_o - \cos \alpha_o) Fn + Z^2 (1 - \cos^2 \alpha_o)$$
$$= \left[(\rho_o + r_o)^2 - R^2 \right] \sin^2 \alpha_o$$

$$-(Fn)^2 \sin^2 \alpha_o + Z^2 \sin^2 \alpha_o = \left[(\rho_o + r_o)^2 - R^2\right] \sin^2 \alpha_o$$

$$Z^2 = (\rho_o + r_o)^2 - R^2 + (Fn)^2$$

$$Z = + \sqrt{(\rho_o + r_o)^2 - R^2 + (Fn)^2}$$

$$\cos \theta = \frac{Fn - Z \cos \alpha_o}{R \sin \alpha} = \frac{Fn - \sqrt{(\rho_o + r_o)^2 - R^2 + (Fn)^2} \cos \alpha_o}{R \sin \alpha_o}$$

$$\cos \theta_{AE} = \frac{Fn - \sqrt{(\rho_o + r_o)^2 - R^2 + (Fn)^2} \cos \alpha_o}{R \sin \alpha_o}$$

Line FE Line FE is the intersection of Zone 2 of the cone with the cylindrical portion of the roller. The cone is:

$$Z = b + \sqrt{b^2 - c}$$

where: $b = \rho_o \sin \alpha_o + F(n-1) \cos \alpha_o$

$$c = (R \cos \alpha_o + \rho_o)^2 + R \sin \alpha_o - F(n-1)^2 - r_o^2$$

And the cylinder is:

$$Z = \frac{1}{\sin \alpha_o} \left\{ R \cos \theta \cos \alpha_o + \sqrt{(r_o + \rho_o)^2 - R^2 \sin^2 \theta} \right\}$$

Solving the equation of the cylinder for cos θ, one proceeds:

$$(r_o + \rho_o)^2 - R^2 \sin^2 \theta = Z \sin \alpha_o - R \cos \theta \cos \alpha_o \quad ^2$$

$$(r_o + \rho_o)^2 - R^2 + R^2 \cos^2 \theta = R^2 \cos^2 \theta \cos^2 \alpha_o + Z^2 \sin^2 \alpha_o$$

$$- 2RZ \cos \theta \sin \alpha_o \cos \alpha_o$$

$$R^2(1 - \cos^2 \alpha_o) \cos^2 \theta + 2 RZ \sin \alpha_o \cos \alpha_o \cos \theta - (Z \sin \alpha_o)^2$$

$$- R^2 + (r_o + \rho_o)^2 = 0$$

$$\cos \theta = \frac{-RZ \sin \alpha_o \cos \alpha_o + \sqrt{(RZ \sin \alpha_o \cos \alpha_o)^2 - R^2 \sin^2 \alpha_o \left[(r_o + \rho_o)^2 - R^2 - (Z \sin \alpha_o)^2\right]}}{R^2 \sin^2 \alpha_o}$$

$$\cos \theta = \frac{-Z \cos \alpha_o + \sqrt{(Z \cos \alpha_o)^2 - (\rho_o + r_o)^2 + R^2 + Z^2 \sin^2 \alpha_o}}{R \sin \alpha_o}$$

$$\cos \theta = \frac{-Z \cos \alpha_o + \sqrt{Z^2 + R^2 - (\rho_o + r_o)^2}}{R \sin \alpha_o}$$

where: $Z = b + \sqrt{b^2 - c}$

$b = \rho_o \sin \alpha_o + F(n-1) \cos \alpha_o$

$c = (R \cos \alpha_o + \rho_o)^2 + [R \sin \alpha_o - F(n-1)]^2 - r_o^2$

Line FA $\theta = 0$

After defining the equations of the line ABCDEFA, the intersection points A, B, C, D, E, F of these lines are to be defined. The radius (R) of these points will be determined. From either of the two equations of the lines passing through any of these points and its radius (R), the angle θ can later be computed.

Point A: $R_A = Fn \sin \alpha_o - (r_o + \rho_o) \cos \alpha_o$

Point B: $R_B = Fn \sin \alpha_o - \rho_o \cos \alpha_o$ (21)

Point C: The value of the radius R_C can be solved from the intersection of the circle BC with Zone 3 of the cone.

Equation (19) of Zone 3, transformed to (x,y,z) axis, will become:

$$Z = F(n-1)\cos \alpha_o + \rho_o \sin \alpha_o + r_o = -x \sin \alpha_o + z \cos \alpha_o + Fn \cos \alpha_o$$

The intersection of Zone 3 with the circle, for which $z = r_o \cos \alpha_o$, will give:

$$F(n-1)\cos \alpha_o + \rho_o \sin \alpha_o + r_o = -x \sin \alpha_o + r_o \cos^2 \alpha_o + Fn \cos \alpha_o$$

$$-F \cos \alpha_o + \rho_o \sin \alpha_o + r_o (1-\cos^2 \alpha_o) = - x \sin \alpha_o$$

$$\therefore \quad x = \frac{1}{\sin \alpha_o} (F \cos \alpha_o - \rho_o \sin \alpha_o - r_o \sin^2 \alpha_o)$$

$$x = F \cot \alpha_o - (\rho_o + r_o \sin \alpha_o)$$

And from the equation of the circle BC, one gets

$$y^2 = (\rho_o + r_o \sin \alpha_o)^2 - x^2$$

Point C in(x,y,z) axis is defined by

$$\begin{cases} x = F \cot \alpha_o - (\rho_o + r_o \sin \alpha_o) \\ y^2 = (\rho_o + r_o \sin \alpha_o)^2 - x^2 \\ z = r_o \cos \alpha_o \end{cases}$$

From the transformation equation (13), one gets

$$R \cos \theta = x \cos \alpha_o + z \sin \alpha_o + Fn \sin \alpha_o$$

$$R \sin \theta = y$$

$$\therefore \quad R^2 = (x \cos \alpha_o + z \sin \alpha_o + Fn \sin \alpha_o)^2 + y^2$$

$$R_C = \sqrt{(x \cos \alpha_o + z \sin \alpha_o + Fn \sin \alpha_o)^2 + y^2}$$

where:

$$x = F \cot \alpha_o - (\rho_o + r_o \sin \alpha_o)$$

$$y = (\rho_o + r_o \sin \alpha_o)^2 - x^2$$

$$z = r_o \cos \alpha_o$$

Point D R_D is defined by the intersection of lines θ_{ED} and θ_{CD}

Point E R_E is defined by the intersection of either two of the three lines: θ_{FE}, θ_{ED} and θ_{AE}.

Point F $R_F = F(n-1) \sin \alpha_o - (\rho_o + r_o) \cos \alpha_o$.

Up to now, n indicated the position of the roller. For practical applications, a term whose physical meaning is easier to visualize should be used. Let the radius R of point A be used, and denoted by R_o:

$$R_o = R_A = Fn \sin \alpha_o - (r_o + \rho_o) \cos \alpha_o$$

$$\therefore \quad Fn = \frac{1}{\sin \alpha_o} \left[R_o + (r_o + \rho_o) \cos \alpha_o \right]$$

This value of Fn is to be inserted wherever it appears.

It is now appropriate to discuss the deflection of the neglected zones.

1. The Zone over Line BC, $(R>R_{BC})$

The difference between a perfect disc and the actual shape of Zone 3 of the cone diminishes rapidly as R increases over R_B. Therefore, neglecting the plastic deformation work on this zone is justified.

2. Lines CD, DE, EF

The actual strain rate is finite and thus does not confirm with our picture (Fig. 12). The strain-rate field is as described except on that line and very close to it. Therefore the work under the area of contact is computed correctly. The work at the discussed zone (line CDEF) is only estimated.

The velocity and strain-rates field

From the equations of the roller, one can compute the values of the following terms:

$$U_z = N \cdot \left[2\pi \cdot \frac{\partial Z}{\partial \theta} + \frac{\partial Z}{\partial n} \right] \qquad (22)$$

$$\dot{\epsilon}_{RZ} = \frac{1}{2} \frac{\partial U_z}{\partial R} \qquad (22)$$

$$\dot{\epsilon}_{\theta z} = \frac{1}{2R} \frac{\partial U_z}{\partial \theta}$$

These terms are long and bulky. Further, under the torus they are expressed as functions of R, θ, Z and n while z is implicitly deduced from the equation of the torus. Altogether, it is possible by the use of these equations and double integration by numerical methods to solve for the work of deformation. But as this requires much labor, some approximations will be made which will not affect the results appreciably and be less laborious.

SOLVING THE POWER BY THE DEFORMATION THEORY

Let a hypothetical cubic block of unit length be exposed to a pure shear.

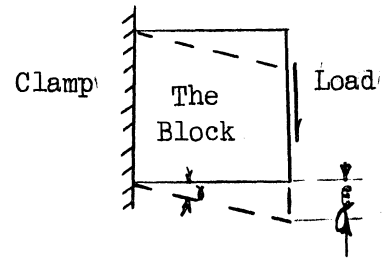

Let the load be $k = \frac{\sigma_o}{\sqrt{3}}$, and the shear angle be γ. The distance traveled is $\delta = 1 \cdot \tan \gamma = \tan \gamma$, and the external work of deformation is $W = k \tan \gamma = \frac{\sigma_o}{\sqrt{3}} \tan \gamma$. This is the work of deformation for a unit volume.

The volume worked on the cone is

$$v = 2\pi RN \, S_o \, F \sin \alpha_o \quad \left[\frac{\text{Inch}^3}{\text{Min}} \right]$$

and the relation between α_o and the shear angle γ is $\gamma = 90^o - \alpha_o$. One can now write the power for the spinning of a cone as

$$\dot{W} = 2\pi RN\, S_o\, F \sin\alpha_o \frac{\sigma_o}{\sqrt{3}} \tan\gamma$$

$$\dot{W} = \frac{2}{\sqrt{3}}\, \pi\, \sigma_o\, RN\, S_o\, F \sin\alpha_o \cot\alpha_o$$

$$\dot{W} = \frac{2}{\sqrt{3}}\, \pi\, \sigma_o\, S_o\, N\, F\, R \cos\alpha_o$$

Let now the same approach be introduced to compute the power for spinning of strain-hardened materials.

Let the strain-stress curve and the shear angle and displacement be described as below.

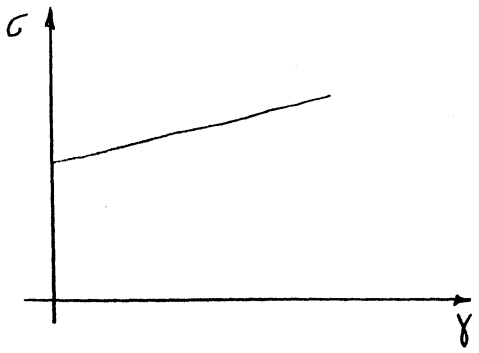

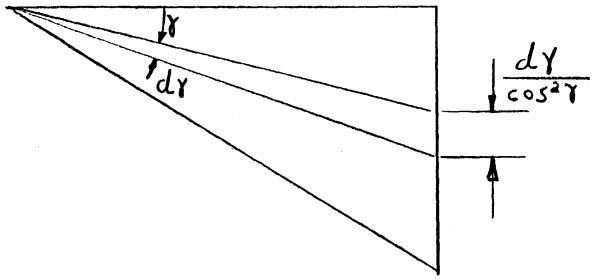

The work per unit volume will be

$$w = \int_{\gamma=0}^{\gamma} \sigma \frac{d\gamma'}{\cos^2\gamma'} \qquad (23)$$

Let the stress-strain curve be approximated by the straight line

$$\sigma = \frac{\sigma_o}{\sqrt{3}} + b\gamma;$$

the integral then becomes

$$w = \int_{\gamma=0}^{\gamma} \left(\frac{\sigma_o}{\sqrt{3}} + b\gamma' \right) \frac{d\gamma'}{\cos^2\gamma'} = \frac{\sigma_o}{\sqrt{3}} \int_{\gamma=0}^{\gamma} \frac{d\gamma'}{\cos^2\gamma'} + b \int_{\gamma=0}^{\gamma} \frac{\gamma' d\gamma'}{\cos^2\gamma'}$$

$$w = \frac{\sigma_o}{\sqrt{3}} \tan\gamma + b \left(\gamma' \tan\gamma' + \ln\cos\gamma' \right) \Big|_0^{\gamma} = \frac{\sigma_o}{3} \tan\gamma + b\left[\gamma \cdot \tan\gamma + \ln(\cos\gamma)\right]$$

And substituting $\gamma = \frac{\pi}{2} - \alpha_o$ one gets:

$$w = \frac{\sigma_o}{\sqrt{3}} \cot\alpha_o + b\left[\left(\frac{\pi}{2} - \alpha_o\right) \cot\alpha_o + \ln(\sin\alpha_o)\right]$$

This is the work per unit volume. To find the power, one multiplies the work per unit volume by the volume machined per minute.

$$\dot{W} = 2\pi RN\, S_o\, F \sin\alpha_o \left\{ \frac{\sigma_o}{\sqrt{3}} \cot\alpha_o + b\left[\left(\frac{\pi}{2} - \alpha_o\right) \cot\alpha_o + \ln(\sin\alpha_o)\right] \right\}$$

Summarizing the results for perfect plastic material and linearly strain-hardened material, one gets

$$\left.\begin{aligned} \dot{W} &= \frac{2}{\sqrt{3}} \pi\, \sigma_o\, S_o\, N\, F\, R \cos\alpha_o \quad - \text{ for perfectly plastic material} \\ \dot{W} &= \frac{2}{\sqrt{3}} \pi\, \sigma_o\, S_o\, NFR \cos\alpha_o + 2\pi\, \sigma_o\, S_o\, NFR\, b\left[\left(\frac{\pi}{2} - \alpha_o\right)\cos\alpha_o + \sin\alpha_o \ln(\sin\alpha_o)\right] \end{aligned}\right\} \quad (24)$$

For linearly strain-hardened material where: $\sigma = \frac{\sigma_o}{\sqrt{3}} + b\,\gamma$.

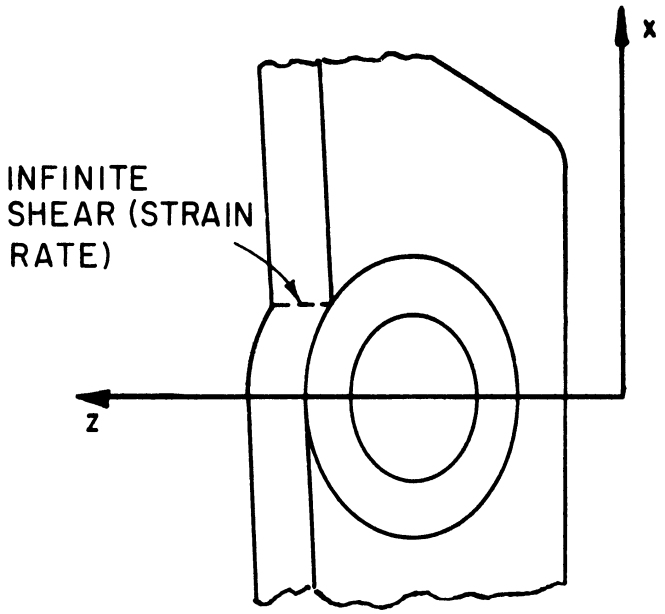

Fig. 12 - The boundary CDEF

SIMPLIFYING THE EQUATIONS FOR NUMERICAL EVALUATION

Repeating here Eq. (11) for the power of plastic deformation (by the incremental theory),

$$\dot{W} = \frac{\sigma_o S_o}{\sqrt{3}} \int_\theta \int_R R \sqrt{\left(\frac{\partial U_z}{\partial R}\right)^2 \left(\frac{1}{R} \cdot \frac{\partial U_z}{\partial \theta}\right)^2}\, dR d\theta \qquad (11)$$

Let a weighted power $(\dot{W}')$ be defined such that

$$\dot{W}' = \frac{\dot{W}\sqrt{3}}{\sigma_o S_o N} \quad \text{and} \quad \dot{W} = \frac{\sigma_o S_o}{\sqrt{3}} N \dot{W}' ; \qquad (25)$$

then the weighted power is:

$$\dot{W}' = \frac{1}{N} \int_\theta \int_R R \sqrt{\left(\frac{\partial U_z}{\partial R}\right)^2 \left(\frac{1}{R} \cdot \frac{\partial U_z}{\partial \theta}\right)^2}\, dR d\theta \qquad (26)$$

Let $\Gamma = \left(\frac{\dot{\epsilon}_{\theta Z}}{\dot{\epsilon}_{RZ}}\right)^2 = \left[\frac{\partial U_z}{R\partial\theta} \Big/ \frac{\partial U_z}{\partial R}\right]^2$ so that the equation for the weighted power can be written:

$$\dot{W}_i' = \frac{2}{N} \int_\theta \int_R R \sqrt{\dot{\epsilon}_{RZ}^2 + \dot{\epsilon}_{\theta Z}^2}\, dR d\theta = \frac{2}{N} \int_\theta \int_R R\sqrt{1+\Gamma}\, \dot{\epsilon}_{RZ}\, dR d\theta \qquad (27)$$

The work of deformation done by the cylindrical portion of the roller will not be computed. The duty of this cylindrical portion is to smooth out the feed mark (Fig. 13). These feed marks are minor in size as the following example of a practical case shows.

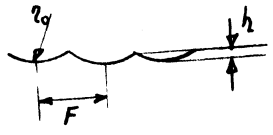

Fig. 13
Feed Marks

$$h = r_o - \sqrt{r_o^2 - \frac{F}{2}^2}$$

For example, if r_o = .250 in. and F = .040 in, one gets

$$h = .250 - \sqrt{.250^2 - .020^2} = .008 \text{ in.},$$

and when reducing F to a half or F = .020 in., one gets

$$h = .250 - \sqrt{.250^2 - .010^2} = .002 \text{ in.}$$

The amount of the displacement caused by the cylindrical portion of the roller is thus neglected. (The work of deformation caused by the cylindrical portion was computed for a number of cases, and found to be negligible. This part of the work is not included in the report). From here on the equations deal only with the torical portion of the roller.

It is to be expected that ζ is a function of R and θ. For $\theta = 0$, one gets $\zeta = 0$. For simplicity, and to be able to perform an integration, it will be assumed that ζ is independent of R and of θ. The constant value of ζ will be chosen arbitrarily as that of ζ at the point E. The distribution of ζ as well as that of $\dot{\epsilon}_{RZ}$ and $\dot{\epsilon}_{\theta Z}$ along line $R = R_B$ and along line ED are given in Table VIII.

INTEGRATING THE POWER

Assuming ζ to be a constant, one can take the square root outside of the integral and Eq. (27) becomes:

$$\dot{W}' = \frac{2}{N} \cdot \sqrt{1+\delta} \int_R \int_\theta R\, \dot{\epsilon}_{RZ}\, dR d\theta = \frac{1}{N} \sqrt{1+\delta} \int_\theta \left[\int_R R \frac{\partial U_z}{\partial R}\, dR \right] d\theta$$

One can perform the integration $\int R \frac{\partial U_z}{\partial R}\, dR$ by substituting $R = U$ and $\frac{\partial U_z}{\partial R}\, dR = dv$.

But a close check of the equation reveals that, while $\frac{\partial U_z}{\partial R}$ is changing appreciably for every minor change in R, R itself can be regarded as constant $R = R_o$.

So: $$\int R \frac{\partial U_z}{\partial R}\, dR \approx R_o \int \frac{\partial U_z}{\partial R}\, dR = R_o \Delta U_z$$

The weighted power becomes

$$\dot{W}' = \frac{\sqrt{1+\delta}}{N} R \int \Delta U_z d\theta \qquad (28)$$

Recalling that

$$U_z = N \left[2\pi \frac{\partial Z}{\partial \theta} + \frac{\partial Z}{\partial n} \right]$$

Let:
$$\left.\begin{aligned} U_{ZP} &= 2\pi N \frac{\partial Z}{\partial \theta} \\ U_{ZC} &= N \frac{\partial Z}{\partial n} \end{aligned}\right\} \qquad (29)$$

and thus:
$$\left.\begin{aligned} \Delta U_z &= \Delta U_{ZP} + \Delta U_{ZC} \\ \Delta U_{ZP} &= 2\pi N \Delta \frac{\partial Z}{\partial \theta} \\ \Delta U_{ZC} &= N \cdot \Delta \frac{\partial Z}{\partial n} \end{aligned}\right\}$$

Let: The total weighted power $\dot{W}^1 = \dot{W}_p^1 + \dot{W}_c^1$

where: the partial power is $\dot{W}_p' = \frac{\sqrt{1+\varsigma}}{N} R_o \int_\theta \Delta U_{ZP} d\theta$

and the complementary power is $\dot{W}_c' = \frac{\sqrt{1+\varsigma}}{N} R_o \int_\theta \Delta U_{ZC} d\theta$

B. COMPUTING THE PARTIAL POWER

$$\dot{W}_p' = \frac{\sqrt{1+\varsigma}}{N} R_o \int \Delta U_{ZP} d\theta = \sqrt{1+\varsigma}\, R_o\, 2\pi \int \Delta \frac{\partial Z}{\partial \theta} d\theta$$

$$\dot{W}_p' = 2\pi R_o \cdot \sqrt{1+\varsigma}\ \Delta Z$$

where: the total $\Delta Z = F \cos \alpha_o$,

and therefore

$$\dot{W}_p' = 2\pi R_o \cdot \sqrt{1+\varsigma}\ F \cos \alpha_o \qquad (30)$$

The similarity of this partial power to the power computed by the deformation theory is to be noticed. For $\varsigma = 0$, $\dot{W}_p$ is the work of deformation computed by the deformation theory, Eq. (20).

C. COMPUTING THE COMPLEMENTARY POWER

The complementary power is

$$\dot{W}_c' = \frac{\sqrt{1+\varsigma}}{N} R_o \int \Delta U_{ZC} d\theta = \sqrt{1+\varsigma}\, R_o \int \Delta \frac{\partial Z}{\partial n} d\theta \qquad (31)$$

The value of $\frac{\partial Z}{\partial n}$ can be evaluated from Eq. (14), G = 0, of the torus. However, an approximate expression that will be as good for numerical evaluation can be developed.

Let the torus be of infinite radius (ρ'_o) (see Fig. 14).

The torus which is now a cylinder as described by the circle of radius r_o is

$$(a - z)^2 + (b - x)^2 = r_o^2$$

$$a - z = \pm \sqrt{r_o^2 - (b - x)^2}$$

$$z = a \mp \sqrt{r_o^2 - (b - x)^2}$$

$$Z = a + \sqrt{r_o^2 - (b - x)^2} = a + \sqrt{r_o^2 - (b - R\cos\theta)^2}$$

$$Z = Fn\cos\alpha_o + \rho_o \sin\alpha_o + \sqrt{r_o^2 - [R\cos\theta - (Fn\sin\alpha_o - \rho_o\cos\alpha_o)]^2} \qquad (32)$$

Deriving Z with respect to n, one gets

$$\frac{\partial Z}{\partial n} = F\cos\alpha_o + \frac{[R\cos\theta - (Fn\sin\alpha_o - \rho_o\cos\alpha_o)] \cdot F\sin\alpha_o}{\sqrt{r_o^2 - [R\cos\theta - (Fn\sin\alpha_o - \rho_o\cos\alpha_o)]^2}}$$

One notices that: $\Delta \frac{\partial Z}{\partial n} = \frac{\partial Z}{\partial n}(R_o) - \frac{\partial Z}{\partial n}(R_o)$

And therefore:

$$\Delta \frac{\partial Z}{\partial n} = F\sin\alpha \left\{ \frac{R_u\cos\theta - (Fn\sin\alpha_o - \rho_o\cos\alpha_o)}{\sqrt{r_o^2 - [R_u\cos\theta - (Fn\sin\alpha_o - \rho_o\cos\alpha_o)]^2}} - \right.$$

$$\left. \frac{R_l\cos\theta - (Fn\sin\alpha_o - \rho_o\cos\alpha_o)}{\sqrt{r_o^2 - [R_l\cos\theta - (Fn\sin\alpha_o - \rho_o\cos\alpha_o)]^2}} \right\}$$

where subscripts u denotes upper bound of integration and

l denotes lower bound of integration.

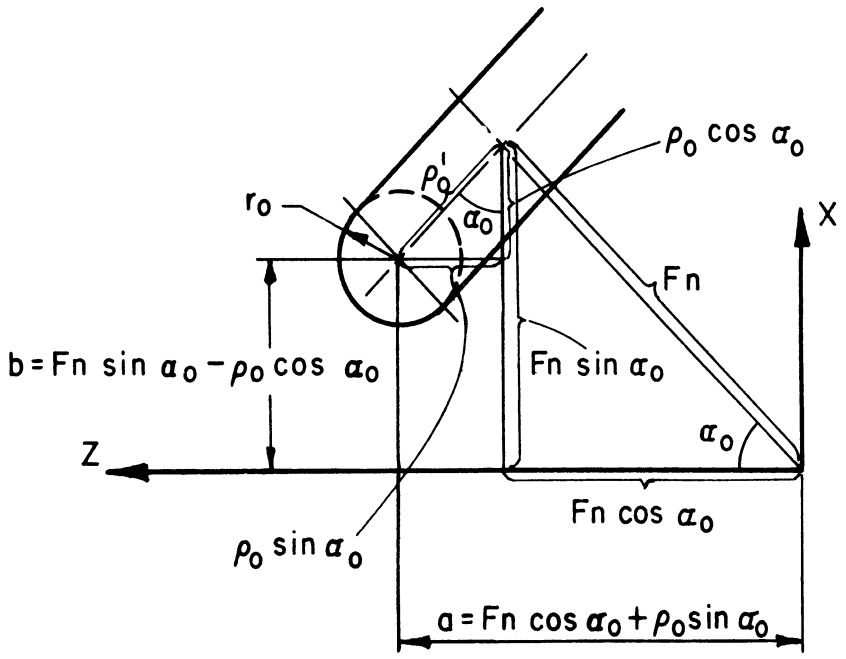

Fig 14 - Approximating the torus by a cylinder

And so, Eq. (31) for the complementary power becomes

$$\dot{W}_c' = \sqrt{1+\delta}\, R_o F \sin\alpha_o \cdot \int_{\text{Boundary of the area of contact}} \left\{ \frac{R_u \cos\theta - (Fn \sin\alpha_o - \rho_o \cos\alpha_o)}{\sqrt{r_o^2 - [R_u\cos\theta - (Fn \sin\alpha_o - \rho_o \cos\alpha_o)]^2}} - \frac{R_1\cos\theta - (Fn \sin\alpha_o - \rho_o \cos\alpha_o)}{\sqrt{r_o^2 - [R_1\cos\theta - (Fn \sin\alpha_o - \rho_o \cos\alpha_o)]^2}} \right\} d\theta \qquad (33)$$

These integrals can be transformed to take the form of elliptic integrals, for which there is a standard procedure for a solution.[4] However, because the boundaries of integration have to be found by a numerical method (namely, a computer), it was found advantageous to do the integration on the computer also.

D. EVALUATING THE STRAIN-RATES RATIO

Let the approximated torus be used [Eq. (32)]:

$$Z = Fn \cos\alpha_o + \rho_o \sin\alpha_o + \sqrt{r_o^2 - [R\cos\theta - (Fn \sin\alpha_o - \rho_o \cos\alpha_o)]^2}$$

The velocity is

$$\frac{U_z}{N} = \frac{1}{N}\frac{dz}{dt} = F\cos\alpha_o - \frac{[R\cos\theta - (Fn \sin\alpha_o - \rho_o\cos\alpha_o)][-R\sin\theta 2\pi - F\sin\alpha_o]}{\sqrt{r_o^2 - [R\cos\theta - (Fn\sin\alpha_o - \rho_o\cos\alpha_o)]^2}} \qquad (34)$$

And evaluating $\frac{1}{N}\frac{\partial U_z}{\partial R}$ and $\frac{1}{N}\frac{\partial U_z}{\partial \theta}$, one continues:

Let: $\dfrac{(Fn \sin\alpha_o - \rho_o \cos\alpha_o) = \beta}{\sqrt{r_o^2 - [R\cos\theta - (Fn\sin\alpha_o - \rho_o\cos\alpha_o)]^2}} = \sqrt{r_o^2 - (R\cos\theta - \beta)^2} = \sqrt{\psi}$

Thus the derivative of $\frac{U_z}{N}$ from Eq. (34) with respect to R becomes:

$$\frac{1}{N}\frac{\partial U_z}{\partial R} = \frac{1}{\sqrt{\psi}}\left\{\cos\theta\left[2\pi R\sin\theta + F\sin\alpha_o\right] + (R\cos\theta - \beta)\,2\pi\sin\theta + \frac{(R\cos\theta-\beta)^2(2\pi R\sin\theta + F\sin\alpha_o)\cos\theta}{(\sqrt{\psi})^2}\right\}$$

$$\frac{1}{N}\frac{\partial U_z}{\partial R} = \frac{1}{(\sqrt{\psi})^3}\left\{\cos\theta\,(2\pi R\sin\theta + F\sin\alpha_o)\left[(\sqrt{\psi})^2 + (R\cos\theta-\beta)^2\right] + (R\cos\theta-\beta)\,2\pi\sin\theta\,(\sqrt{\psi})^2\right\}$$

$$\frac{1}{N}\frac{\partial U_z}{\partial R} = \frac{1}{(\sqrt{\psi})^3}\left\{r_o^2\cos\theta\,(2\pi R\sin\theta + F\sin\alpha_o) + 2\pi\sin\theta\,(\sqrt{\psi})^2(R\cos\theta-\beta)\right\}$$

And the derivative of $\frac{U_z}{N}$ with respect to θ becomes:

$$\frac{1}{N}\frac{\partial U_z}{\partial\theta} = \frac{1}{\sqrt{\psi}}\left\{R\sin\theta\left[2\pi R\sin\theta + F\sin\alpha_o\right] + \left[R\cos\theta - \beta\right]2\pi R\cos\theta - \frac{(R\cos\theta-\beta)^2\left[2\pi R\sin\theta + F\sin\alpha_o\right]R\sin\theta}{(\sqrt{\psi})^2}\right\}$$

$$\frac{1}{N}\frac{\partial U_z}{\partial\theta} = \frac{1}{(\sqrt{\psi})^3}\left\{-R\sin\theta\left[2\pi R\sin\theta + F\sin\alpha_o\right]\left[(\sqrt{\psi})^2 + (R\cos\theta-\beta)^2\right] + (R\cos\theta-\beta)\,2\pi R\cos\theta\,(\sqrt{\psi})^2\right\}$$

$$\frac{1}{N}\frac{1}{R}\frac{\partial U_z}{\partial\theta} = \frac{1}{(\sqrt{\psi})^3}\left\{-r_o^2\sin\theta\left[2\pi R\sin\theta + F\sin\alpha_o\right] + 2\pi\cos\theta\,(R\cos\theta-\beta)\,(\sqrt{\psi})^2\right\}$$

Recalling that by definition:

$$\int = \left(\frac{\dot{\epsilon}_{\theta Z}}{\dot{\epsilon}_{RZ}}\right)^2 = \left(\frac{\frac{1}{R}\frac{\partial U_z}{\partial \theta}}{\partial U_z/\partial R}\right)^2$$

one gets:

$$\int = \frac{2\pi \cos\theta\,(R\cos\theta - \beta)\,(\sqrt{\psi})^2 - r_o^2 \sin\theta\left[2\pi R \sin\theta + F \sin\alpha_o\right]}{2\pi \sin\theta\,(R\cos\theta - \beta)\,(\sqrt{\psi})^2 + r_o^2 \cos\theta\left[2\pi R \sin\theta + F \sin\alpha_o\right]} \qquad (35)$$

where:

$$\beta = Fn \sin\alpha_o - \rho_o \cos\alpha_o$$

$$\sqrt{\psi} = \sqrt{r_o^2 - [R\cos\theta - (Fn \sin\alpha_o - \rho_o \cos\alpha_o)]^2}$$

THE TANGENTIAL FORCE

The numerical results will be presented in a graphical form. The power is a linear function of the following parameters: yield limit (σ_o), thickness (S_o), and speed in RPM (N). It will therefore be better to introduce a weighed tangential force and plot its dependence on the other process variables. The number of graphs will thus be reduced, and the real tangential force and power can be found from those plots and computed for a variety of materials, thicknesses and speeds.

First it will be shown that the greatest portion of the power is absorbed through the tangential component of the force acting between the roller and the cone. Let the force be resolved to its three following components: Tangential Force (t), Radial Force (F_R) and Feed Force (F_A) (see Fig. 1). The power consumed

can be composed of the total power delivered by these three components of the force separately by each cone. In general, the power is the force multiplied by the velocity directed parallel to this force. (The dot product of the force by the velocity). This can be expressed as

$$\dot{W} = t.S_t + F_A.S_A + F_R.S_R$$

The roller does not move in the radial direction, or $S_R = 0$. It follows that

$$\dot{W} = t.S_t + F_A.S_A = \dot{W}_t + \dot{W}_A$$

where:

$\dot{W}_t = t.S_t$ - The "tangential power"

$\dot{W}_A = F_A.S_A$ - The "feed power"

The "circumferential velocity" is $S_t = 2\pi RN$,

and the feed velocity is $S_A = F \cdot N$

The ratio for the "feed power" to the total power is:

$$\frac{\dot{W}_A}{\dot{W}} = \frac{\dot{W}_A}{\dot{W}_A+\dot{W}_t} = \frac{1}{1+\frac{\dot{W}_t}{\dot{W}_A}} = \frac{1}{1+\frac{2\pi R}{F}\,\frac{t}{S_A}}$$

A typical case follows (see Table VI reading M10).

$F = .028$ inch/R
$R = 1$ inch
$F_A = 1640$ lb
$t = 100$ lb

$$\frac{\dot{W}_A}{\dot{W}} = \frac{1}{1+\frac{2\pi}{.028}\cdot\frac{100}{1640}} = \frac{1}{1+13.7} = \frac{1}{14.7} = .068$$

The power consumed by the "feed force" is about 6.8% of the total power. Let the feed power be neglected and the work consumed be regarded as done entirely by the tangential force. One now gets:

$$\dot{W} = t.S_t = 2\cdot\pi\cdot R\cdot N\cdot t$$

And the tangential force is

$$t = \frac{\dot{W}}{2\pi RN} = \frac{\sigma_o S_o \dot{W}'}{2\sqrt{3}\,\pi R} \text{ lb.}$$

Let a weighed tangential force (t') be introduced such that:

$$t' = \frac{t}{\sigma_o \cdot S_o}$$

Equation (36) summarizes the relations between the power, weighed power, tangential force, and weighed tangential force.

$$\left.\begin{aligned} t &= \frac{\dot{W}}{2\pi RN} = \frac{\sigma_o S_o \dot{W}'}{2\sqrt{3}\,\pi R} = \sigma_o \cdot S_o \cdot t' \\ t' &= \frac{\dot{W}}{2\pi RN\cdot\sigma_o S_o} = \frac{\dot{W}'}{2\sqrt{3}\,\pi R} = \frac{t}{\sigma_o S_o} \\ \dot{W} &= \frac{\sigma_o \cdot S_o}{\sqrt{3}} N\dot{W}' = 2\pi RN\sigma_o S_o t' = 2\pi RNt \\ \dot{W}' &= 2\sqrt{3}\,\pi Rt' = \frac{2\sqrt{3}\,\pi R}{\sigma_o S_o} t = \frac{\sqrt{3}}{\sigma_o S_o N} \dot{W} \end{aligned}\right\} \quad (36)$$

THE EXPERIMENTAL WORK

Two types of experiments were conducted. One was designed to study the nature of deformation that takes place during the process. The other was designed to measure the forces between the tool and the work during the process.

In usual practice during many spinning operatings, the flange (Zone 3) of the cone is distorted. This distortion is very undesirable because a highly distorted flange cannot be worked into a cone and the operation stops or the cone is cracked. This distortion is discussed in Refs. 2, 5, and 6, and some explanations of the factors governing this distortion are given.

It was experienced in this study that the predominant factor governing distortion is the thickness S_1 of the cone. The thickness of all cones spun and analyzed in this study was kept uniform and according to the equation $S_1 = S_o \sin \alpha_o$, which will be called the "sine law." In this case the flange is always straight and undistorted.

A. THE EXPERIMENTAL DETERMINATION OF THE NATURE OF DEFORMATION

The study of the nature of the deformations took two tracks. One was a study of the microstructure of the deformed cone, the other, of the general pattern of the deformation.

The microstructure study showed that the outer surface of the cone was more deformed than the side facing the mandrel. At the same time higher temperature existed at the outer surface and hence more recrystallization occurred on this side of the cone. These phenomena are discussed in Ref. 5 (p. 6).

The general pattern of the deformations was first studied by putting grid lines on the original disc and then following the direction they took after deformation. The results of this study are given in Ref. 5. This method showed only the displacement pattern over the surface, ignoring the depth. Later a better technique was used, as follows.

In the original disc .0125-in. holes were drilled and plugged with "sculp" metal (see Fig. 16). After the cones were spun, the metal was carefully cut and filed until the holes were revealed. From the direction of the plugs, a three-dimensional deformation picture was constructed. A typical picture of the holes is Fig. 17. This cone was spun and checked by Cincinnati Milling Machine Co. as part of a study conducted there.

A top view on the radial line of holes, shows the shear $\epsilon_{R\theta}$ of the cone (see Fig. 18).

The angle α_θ indicate by how much the outer surface slipped over the inner surface of the cone. A listing of α, $\Delta\alpha_R$ and α_θ for a variety of cones is given in Table V. $\Delta\alpha_R$ was measured at different radial distances on each cone. α_θ was considered to be zero in the analytical study and compared to $(90-\alpha_o)$, which is the main shear, it is seen to be small enough. No explanation has been found of the odd values of $\Delta\alpha_R$, which prevents inclusion of this distortion in the analytical approach.

The analytical approach assumed a pure shear ϵ_{RZ} which means that $\alpha=0$. This assumption does not hold. For big α_o, it seems that the deformation is closer to pure bend. For smaller α_o, the deformation is closer to pure shear

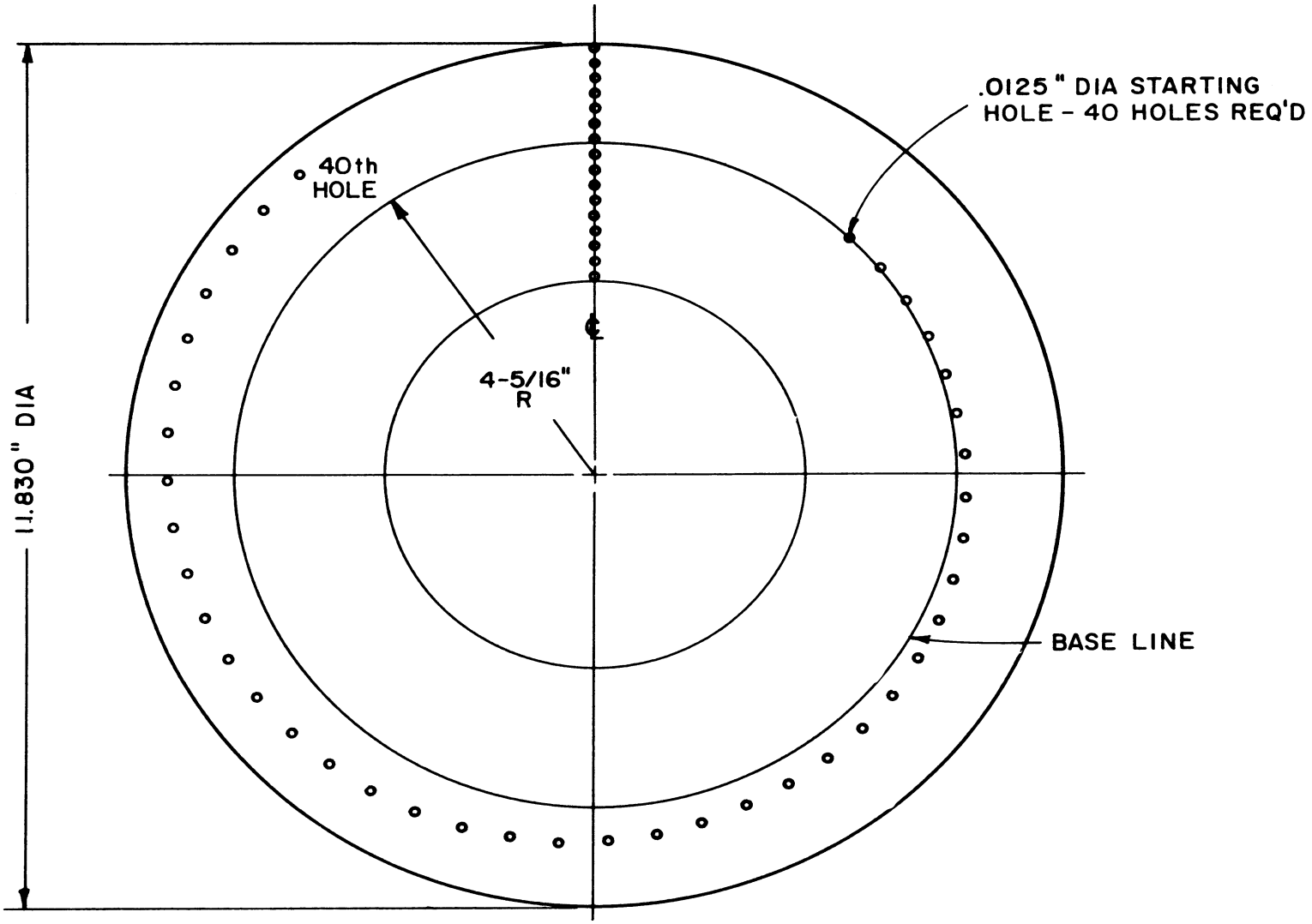

Fig. 16 - Holes in the original disc

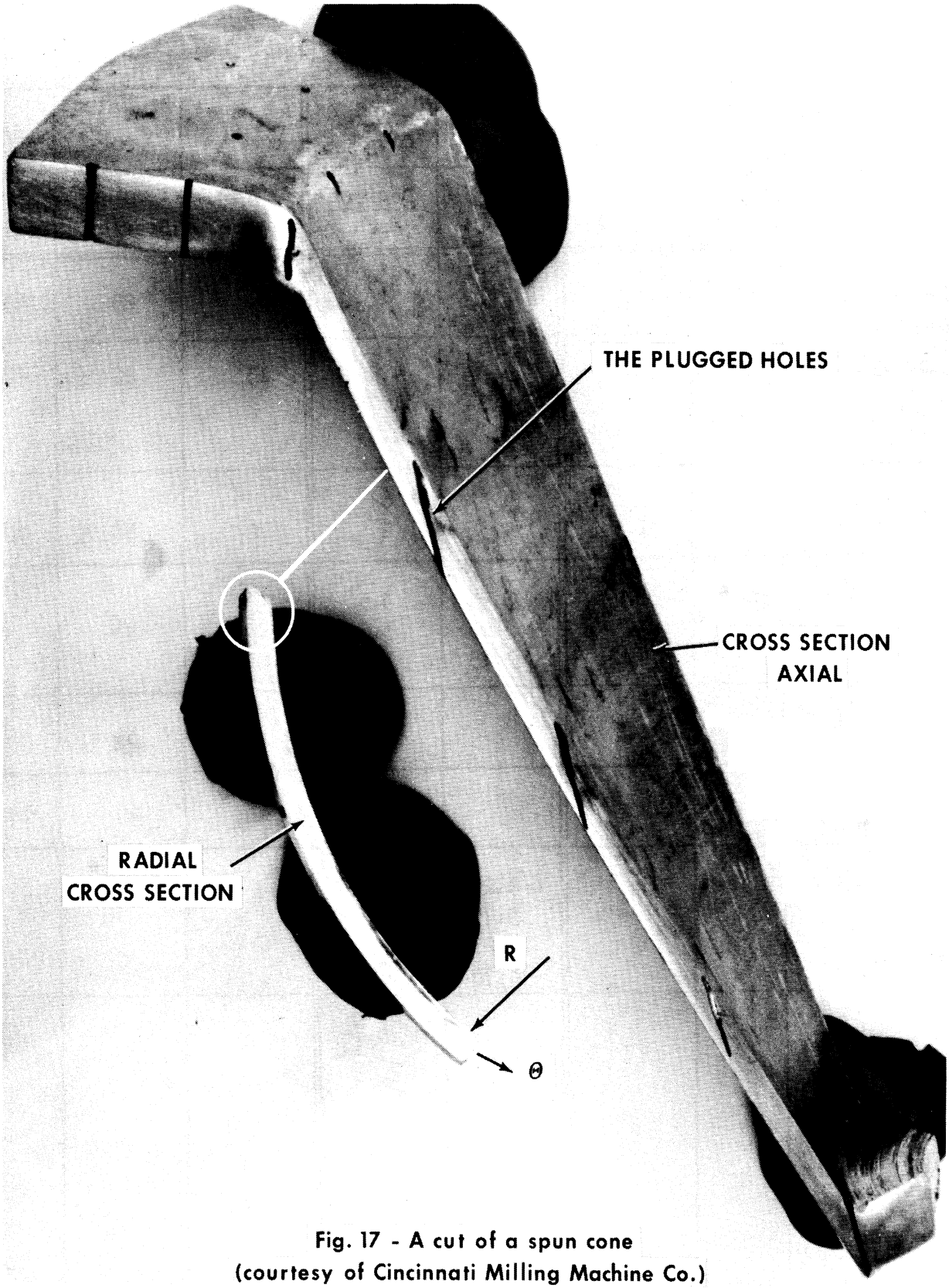

Fig. 17 - A cut of a spun cone
(courtesy of Cincinnati Milling Machine Co.)

Table V - Distortion of Holes Pattern in Spun Cones.

(original thickness S_o = .081")

See Fig. 18

Cone Number	Mat.	Cone Angle, α_o	Radius R	$\Delta \alpha_R$	Average α_Φ	α	$90^o-\alpha$
		Degrees	Inch	$\frac{\text{Degrees}}{\text{inch}}$	Degrees	Degrees	Degrees
1-A-1-R-.5	Al	31.5	4 4.5°	3,5° 0°	6	25	65
1-A-1-R-1	Al	31.5	4 4.5 5	4.5 1.75 2.75	13	22	68
7-A-1-R-.5	Brass	31.5	4 4.5	6 2	12	18	72
9-A-1-R-1	Brass	31.5	3.75 4.25 4.75	3.5 3.5 1.75	17	33	57
1-A-20-R-1	Al	42.5		0	7	35	55
1-A-20-R-5	Al	42.5		0	2	45	45
9-A-3-JJ-R-1	Brass	54	3.25 3.75 4.25 4.75	2 2 3 2	3	23	67

than to bending. It is felt that by assuming pure shear, a computed value for the power will be fairly close to the actual one (see Appendix 2).

B. MEASURING THE POWER AND TANGENTIAL FORCE

This set of experiments was done in two separate places, one at Cincinnati Milling Machine Company, and the other at Spincraft, Incorporated.

Cincinnati Milling Machine Co. was conducting a study of the spinning operation for quite a long time. Equipment, already constructed, consisted of a three-dimensional dynamometer connected to a 3-channel recorder. The roller is mounted on the dynamometer, and thus the force between the roller and the cone is measured. It was agreed that Cincinnati Milling Machine Co. would run a set of tests designed especially to check the analytical approach developed in this study. The results are plotted in Figs. 21, 22, 23, and 24. In this study only the tangential force was analyzed.

At Spincraft the power consumption of the d-c motor, which drives the main spindle, was measured. This was done by recording the voltage and current through the motor (see Fig. 25). The data and experimental results are listed in Table IX. The analytical results, compared with the experimental data, will be given in the next report.

One can write the power consumed by the motor to be:

$$\dot{W}_t = \dot{W}_o + \eta \dot{W}$$

where:

$\dot{W}_t$ is the power measured at load,
$\dot{W}_o$ is the power measured at no load,
$\dot{W}$ is the power of deformation consumed by the cone, and
η is the efficiency factor.

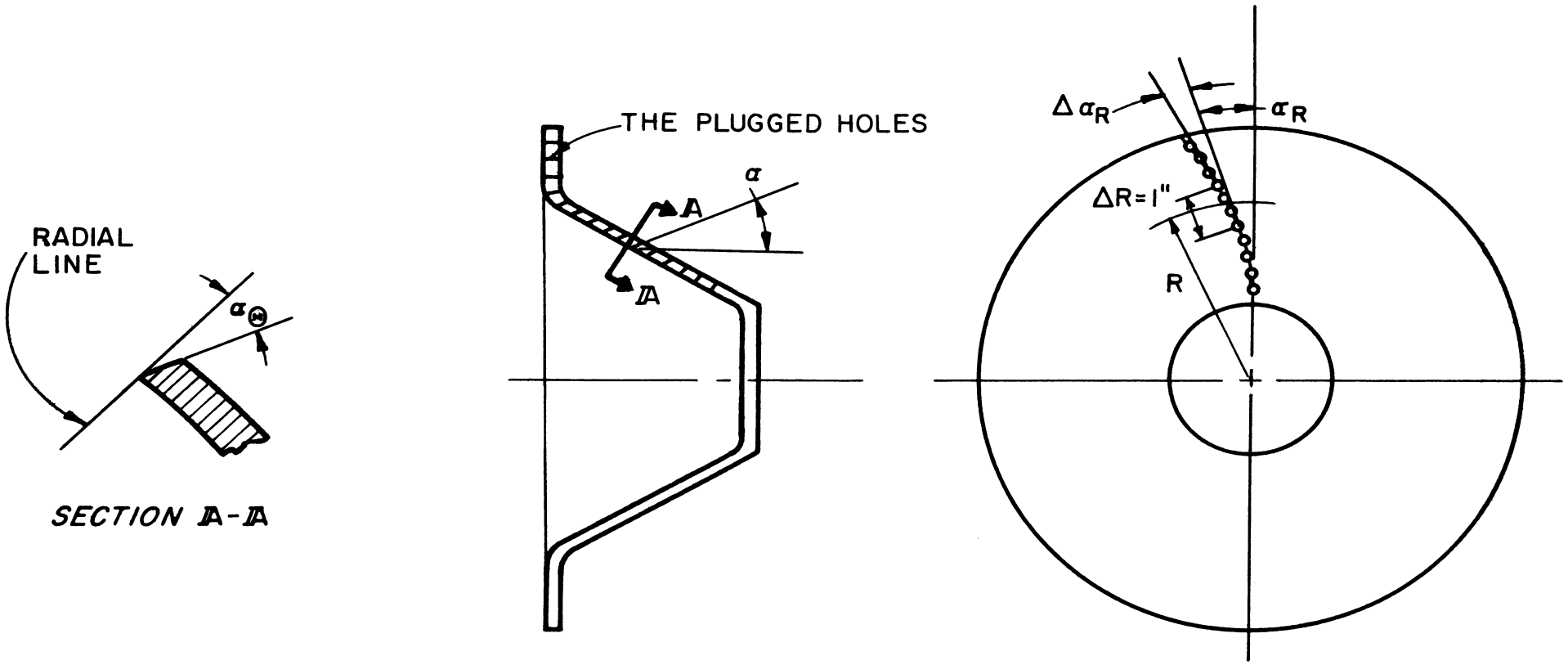

Fig. 18 - Directions of holes in the cone

TABLE VI

Cincinnati Results of Recorded Forces

1	2	3	4	5	6	7	8	9	10	11	12	13	14	15	16	17	18	19	20	21	22	23	24	25	26	27	28	29	30	31	32
	Run Number	Material	Original Thickness	Half Included Angle	Feed per Revolution	Rollers "Round Off"	Rollers Radius	Yield Limit of Worked Cone	Speed				Feed per Minute		Cones Radius		Voltage Drawn		Excess Current Drawn		Power Consumed		Experimental Tangential Force		Weighting Factor		Experimental Weighted Tangential Force				
									Initial	Halfway	Final	Representative			Small	Large	At Small Radius	At Large Radius	At Small Radius	At Large Radius	At Small Radius	At Large Radius	At Small Radius	At Large Radius			At Small Radius	At Large Radius			
			in.	°	ipr	inch		psi	rpm				ipm		inch		volts		amp		lb-in./min		lb		ppi		inch				
			S_o	α_o	F	r_o	ρ_o	σ_o	N_S	N_H	N_F	N	NF		R_1	R_2	V_1	V_2	ΔI_1	ΔI_2	$\dot{W}_1$	$\dot{W}_2$	t_1	t_2			t_1'	t_2'			
																					$\dot{W} = 531{,}000 \cdot V \cdot \Delta I$		$t = \frac{\dot{W}}{2\pi RN}$		$\sigma_o \cdot S_o$		$t' = \frac{t}{\sigma_o \cdot S_o}$				
	M14	1100 Al	.250	35	.021	1/4	7	25000				300	6.3		1.0								75		6250			.012			
	M2	1100 Al	.250	35	.022	1/4	7	25000				300			1.0								50		6250			.008			
	M1	1100 Al	.250	35	.024	1/4	7	25000				300			1.0								95		6250			.015			
	M10	1100 Al	.250	35	.028	1/4	7	25000				300			1.0								100		6250			.016			
	M11	1100 Al	.250	35	.030	1/4	7	25000				300			1.0								120		6250			.019			
	M3	1100 Al	.250	35	.042	1/4	7	25000				300			1.0								130		6250			.021			
	M4	1100 Al	.250	35	.025	1/8	7	25000				300			1.0								155		6250			.025			
	M9	1100 Al	.250	35	.030	1/8	7	25000				300			1.0								120		6250			.019			
	M5	1100 Al	.250	35	.030	1/2	7	25000				300			1.0								105		6250			.017			
	D30I	1100 Al	.375	35	.025	1/4	7	25000				300			1.0								200		9370			.021			
	D42I	1100 Al	.485	35	.033	1/4	7	25000				300			1.0								300		12000			.025			
	M8	1100 Al	.250	21	.028	1/4	7	25000				300			1.0								130		6250			.021			
	M7	1100 Al	.250	21	.033	1/4	7	25000				300			1.0								105		6250			.017			
	M12	1100 Al	.250	21	.035	1/4	7	25000				300			1.0								115		6250			.0185			

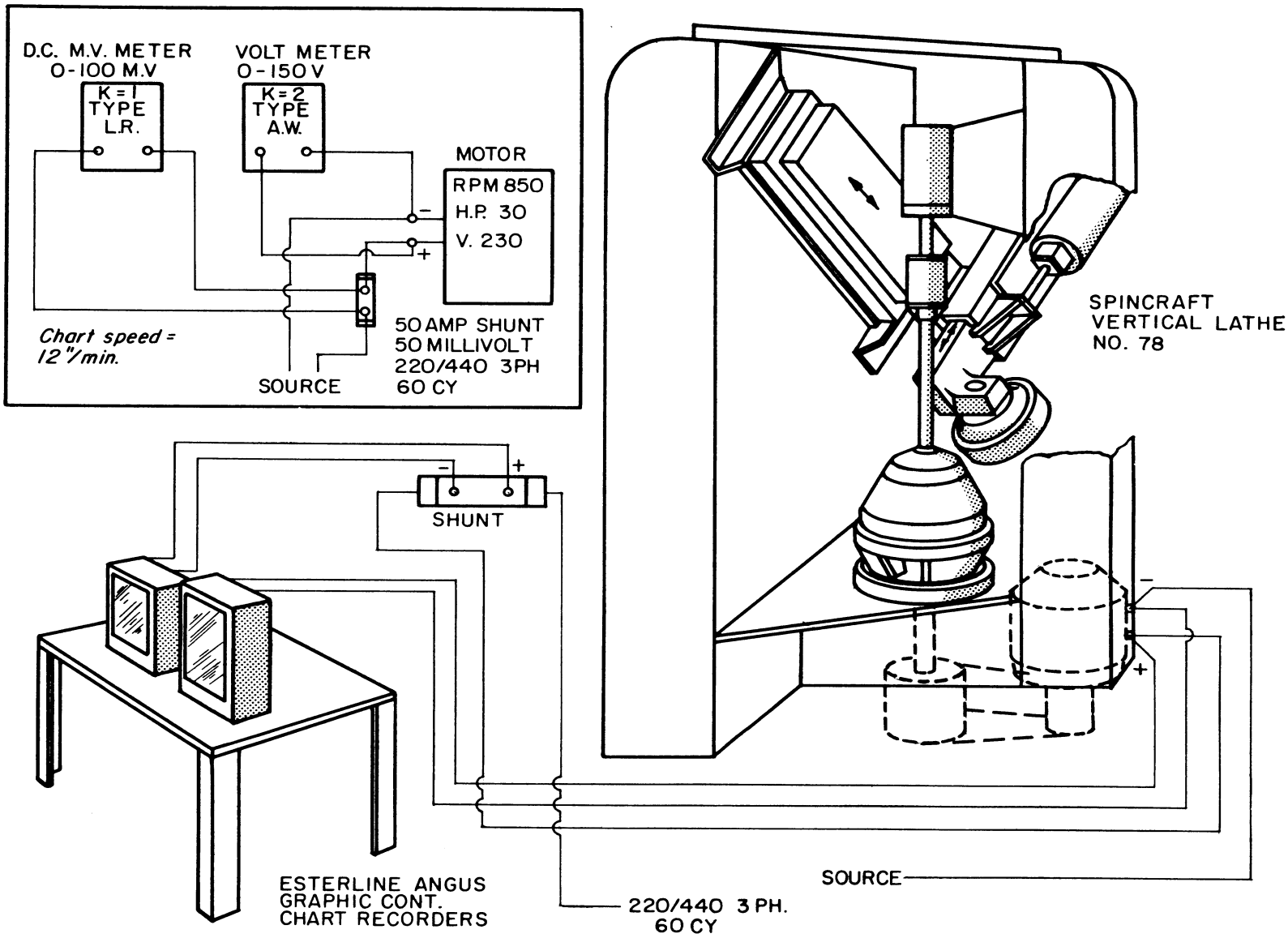

Fig. 25 - Spincraft experimental set up. (Courtesy of Spincraft Inc.)

Table IX with Spincraft experimental data and the plots of Spincraft experimental data against the theoretical answer are not included in this report. These results will follow at a later date. Table VII - computed weighted power and tangential force - and Table VIII - the distribution of strain rates and τ_r are provided under separate cover.

The same equation can be transformed to:

$$\dot{W} = \frac{\dot{W}_t - \dot{W}_o}{\eta}$$

The efficiency η for the experiment at Spincraft was arbitrarily chosen.

For the analytical solution, a value for the uniaxial yield limit is required. From each cone spun in this set of tests, a specimen was cut as Fig. 26 shows, and tested on a tensile test machine. A typical stress-strain curve is shown in Fig. 28. An average stress was chosen to be the yield limit (see Appendix 3).

RESULTS

The nature of the deformations has been discussed in Ref. 5. Table V gives the deformations as had been found by the holes technique. The effects of each of the parameters, Feed F, cone included angle $2\alpha_o$, cone radius R_o, roller "round-off" radius r_o, and roller radius ρ_o on the power and tangential force, are given in the following graphs.

Knowing those five parameters for an actual case, one finds from the suitable graph the value of the weighted tangential force. By a simple computation, the tangential force and power are obtained:

$$t = \sigma_o \cdot S_o \cdot t$$

$$\dot{W} = 2\pi RN\, t = 2\pi RN\sigma_o S_o\, t$$

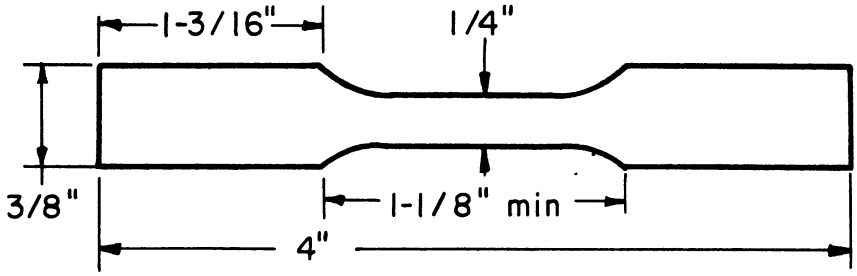

Fig. 26-Specimen for tensile test

where t - the tangential force,

σ_o - yield limit of the actual cone at uniaxial tensile test,

S_o - original disc thickness,

t' - weighted tangential force as found from the graph,

R - radius of cone where the force t is applied, and

N - speed of cone in rpm.

CONCLUSIONS

(1) The aim of this study was to find the power consumed in the mechanical spinning of cones.

The information gathered about the process gave the geometrical picture, and some vague idea about the general pattern of the displacements. For the analytical study, a displacement field was postulated, which gave the strain-rates field and the stress-deviator field. The strain-rate field does satisfy automatically the compatability conditions. Because of the very complicated boundaries, which require numerical methods for determination, no attempt was made to check the stresses for satisfaction of the equations of equilibrium. No load-boundary conditions are given, and therefore no steps were taken to satisfy any load distribution. Only the geometrical boundary conditions are satisfied.

Although the above approach is far from giving a rigorous solution for the stress and strain fields, it does give a fairly good approximation of the required work of deformation.

(2) In addition to the solution by the incremental theory, a solution by the deformation theory was given. It is seen that as the radius (R) of the cone increases, the incremental-theory solution approaches the solution given by the deformation theory.

This is explained by the following reasoning. For the incremental theory, in the numerical solution, it was assumed that the ratio ζ between the two nonzero strain-rate components was constant. This assumption gave a fairly good value for the power. By assuming ζ to be a constant, a "radial load" was postulated. A "radial load" is one in which each component of strain (and stress) increases with time at the same rate as the others. For this load it has been proved that the incremental theory is in complete agreement with the deformation theory.

In the deformation-theory solution, it was assumed that $\epsilon_{R\theta} = 0$. As the radius of the cone R_o grows bigger, the maximum angle θ of point D on the area of contact gets smaller. The circle R = constant approaches the cord on which $\dot{\epsilon}_{R\theta} = 0$. It is therefore to be expected, as R_o grows and $\epsilon_{R\theta}$ approaches zero, that the solution according to the incremental theory will approach that of the deformation theory.

The deformation-theory solution is therefore a good quick way to find the approximate power requirements.

(3) The effect of the parameters on the tangential force can be summarized as follows.

For any set of parameters, the cone is spun from a minimum R_o at the bend to a maximum R_o at the outer radius. As the radius gets bigger, the tangential force is decreased, but never gets less than the tangential force predicted by the deformation theory. Let this minimum tangential force be called the "most efficient process force." Whenever a change of parameters brings the tangential force closer to the minimum, it will be regarded as making the process more efficient.

(a) The tangential force is linearly dependent on the yield limit σ_o and on the blank's thickness, S_o as long as the thickness is much less than the minimum diameter spun.

(b) Increasing the feed (F) will decrease the efficiency.

(c) The minimum tangential force is proportional to $\cos\alpha_o$. The more deformation is introduced (smaller α_o), the worse is the efficiency.

(d) As the roller round-off radius r_o approaches zero, the efficiency approaches its best value. As r_o gets bigger than about $\frac{1}{4}$ in. in practical conditions, a further increase does not change the efficiency very much.

(e) As the roller radius ρ_o approaches zero, the efficiency approaches its best value (see Ref. 2, Part II, p. 255). Here for values of $6" < \rho_o < 10"$ the changes in efficiency are very small.

Each one of the effects mentioned above is more noticeable as R_o gets smaller. For very big R_o, the efficiency is approaching its best value for any value of the other parameters.

(4) For the numerical evaluation of the expression for the power, many approximations were made. The original expression could have been evaluated for the exact form of the roller. This would have required a much more complicated program handled by a bigger machine than the IBM 650. This study was mainly conducted to find a way to evaluate the power and to prove the soundness of this way. The shorter and simpler program proved it.

(5) In the set of tests to find the forces, a dynamometer was used in one case and a power measurement in the other. The tangential force measured by the dynamometer showed a wide spread or irreproducibility. The most likely reasons for that spread are: (a) the conditions might not have been under full control, or (b) the dynamometer might be inaccurate. At any rate, if further tests are to be run, this source of trouble should first be located.

The dynamometer readings were accepted only at the smaller radius R_o = 1 in. As the roller advanced, it started to rub on the flange. In regular operation this rubbing is undesirable and can be eliminated. On any further test, care should be taken to get rid of this rubbing, and have a record of the power for the full length of the operation.

THE EFFECT OF THE FEED (F)
ON THE WEIGHTED TANGENTIAL FORCE t'

– – – – Predicted by the simplified deformation theory

——— Predicted by the incremental theory

o Cincinnati experimental data

$\rho_0 = 7$ in., $r_0 = .250$ in., $\alpha_0 = 35°$

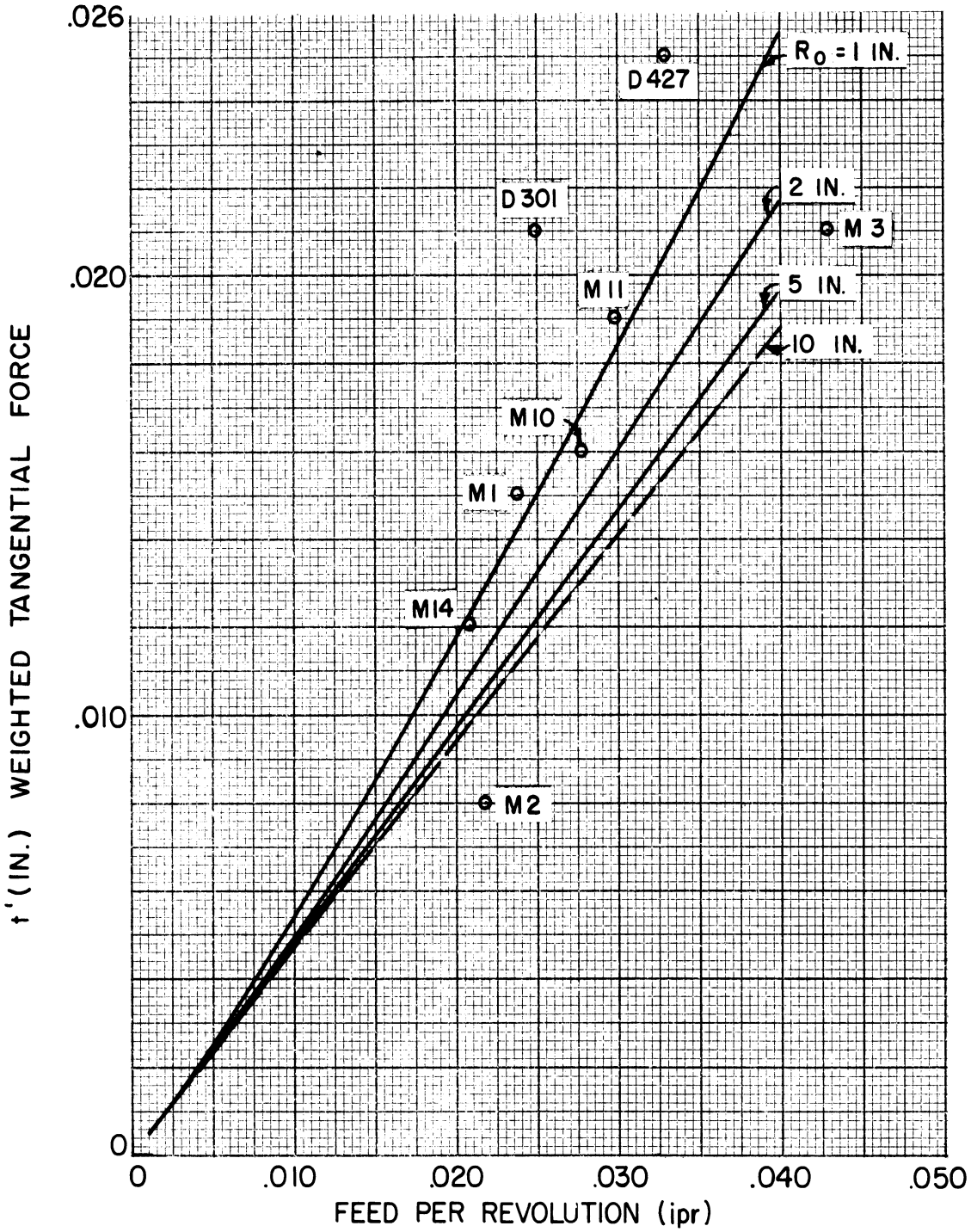

The tangential force $t = \sigma_0 \cdot s_0 \cdot t'$ (lb)

The power $w = 2\pi R_0 N t = 2\pi \cdot \sigma_0 \cdot s_0 \cdot R_0 \cdot N \cdot t' \left(\frac{\text{lb in.}}{\text{min}}\right)$

Fig. 21 – Tangential force vs. feed

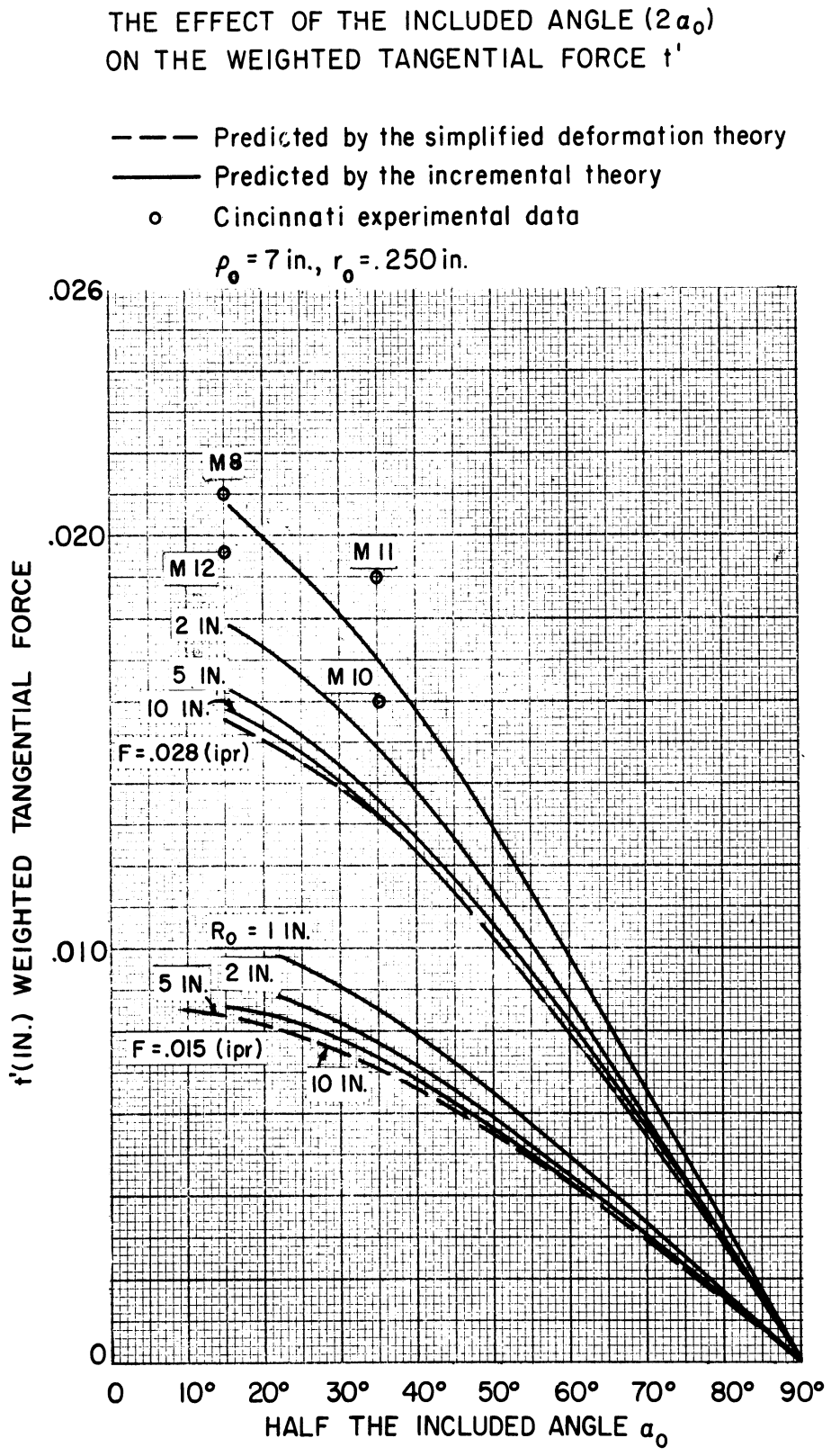

The tangential force $t = \sigma_0 \cdot s_0 \cdot t'$ (lb)

The power $w = 2\pi R_0 N \quad t = 2\pi \cdot \sigma_0 \cdot s_0 \cdot R_0 \cdot N \cdot t' \left(\frac{\text{lb in.}}{\text{min}}\right)$

Fig. 22 - Tangential force vs. included angle

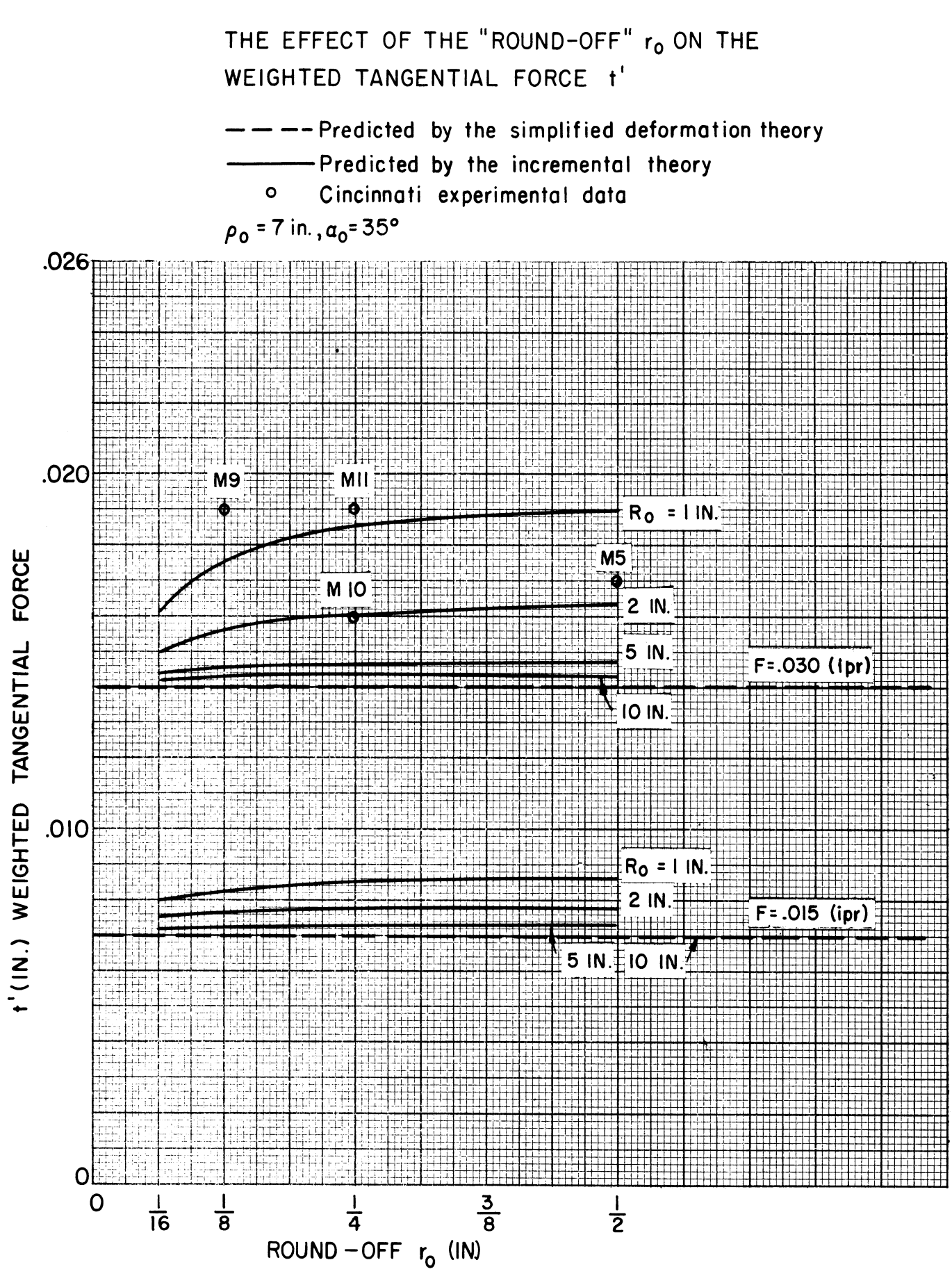

The tangential force $t = \sigma_0 \cdot s_0 \cdot t'$ (lb)

The power $w = 2\pi R_0 N t = 2\pi \sigma_0 \cdot s_0 \cdot R_0 \cdot N \cdot t' (\frac{\text{lb in.}}{\text{min}})$

Fig. 23 - Tangential force vs. "Round off" radius

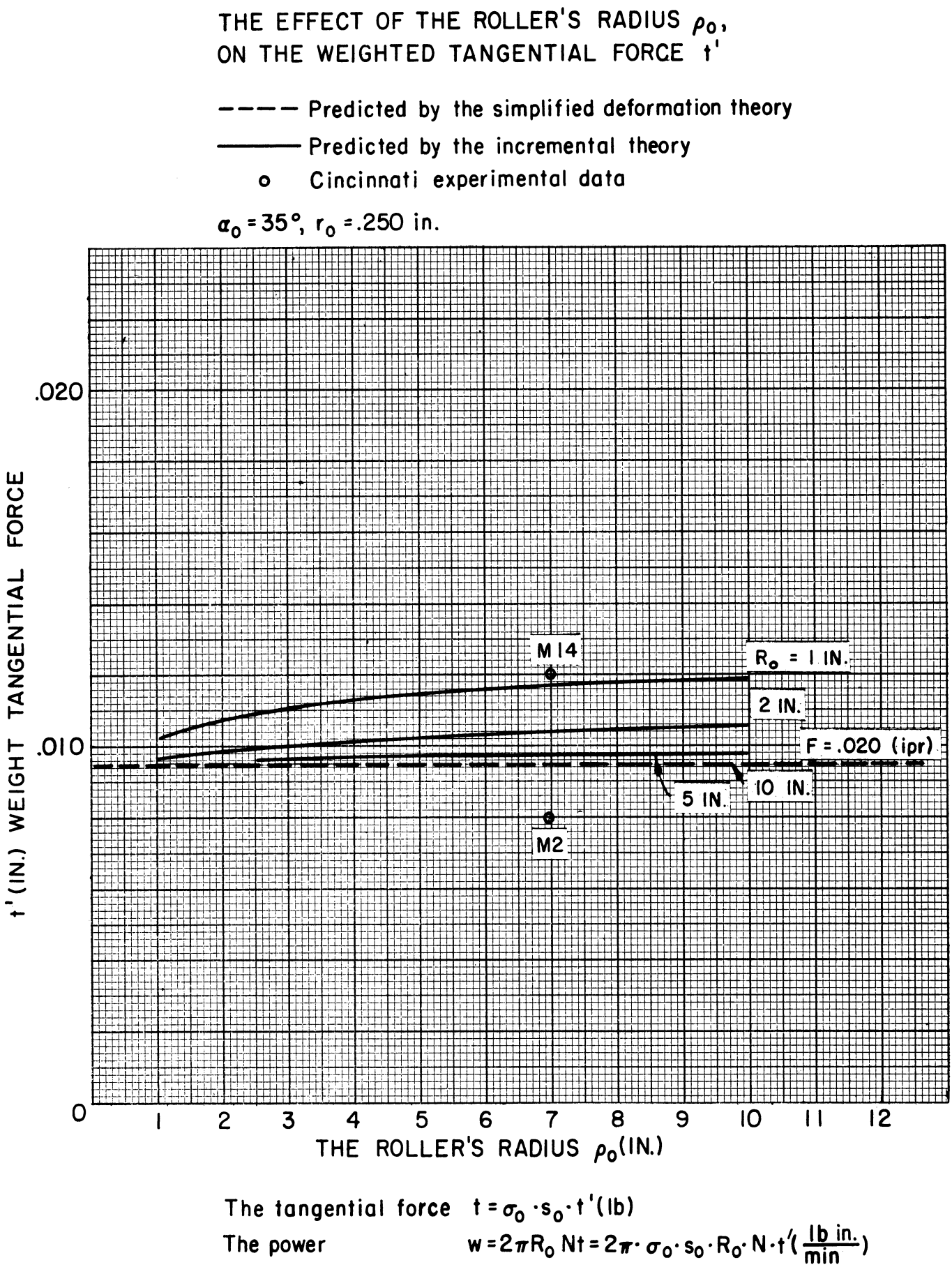

The tangential force $t = \sigma_0 \cdot s_0 \cdot t'$(lb)

The power $w = 2\pi R_0 Nt = 2\pi \cdot \sigma_0 \cdot s_0 \cdot R_0 \cdot N \cdot t'(\frac{\text{lb in.}}{\text{min}})$

Fig. 24 - Tangential force vs. roller's radius

REFERENCES

1. Lengbridge, J., "Economics of Spinning and Drawing," Tool Eng., 30, 89-94 (1953).

2. Reichel, H., "Roll Spinning of Cone Shaped Aluminum Parts," Fertigungstechnik, 8, Part 1, No. 5, 181-184 (April, 1958); Part 2, No. 6, 252-260 (June, 1958).

3. Rouse, H. (Editor), Advanced Mechanics of Fluids (John Wiley and Sons, Inc., New York, 1959), p. 204.

4. Von Karman, T., and Biot, M. A., Mathematical Methods in Engineering (McGraw-Hill Book Co., New York, 1940), pp. 119-130.

5. Avitzur, B., Carleton, W. D., Floreen, S., Hucke, E. E., and Ragone, D. V., Mechanically Spun Cones, Univ. of Michigan Eng. Res. Inst. Report 2621-4-P, Ann Arbor, June, 1958.

6. Feola, J. N., Experimental Analysis of Shear Deformation, unpublished M. S. thesis, Syracuse University, January, 1955.

7. Perlic, A. S. Smith, J. W., and Van Zoeren, H. R., Internal Translator (IT), A compiler for the 650, Univ. of Mich. Statistical Res. Lab., January, 1957.

APPENDIX 1

PROGRAM FOR THE IBM 650 DIGITAL COMPUTER

It now remains to solve numerically the following sets of equations.

From the deformation theory

$$\left.\begin{aligned} \dot{W} &= \frac{2}{\sqrt{3}}\,\pi\sigma_o S_o\, NFR_o \cos\alpha_o \\ \dot{W}' &= 2\pi\, F\, R_o \cos\alpha_o \\ t &= \frac{\sigma_o S_o}{\sqrt{3}}\, F\cos\alpha_o \\ t' &= \frac{F}{\sqrt{3}}\cos\alpha_o \end{aligned}\right\} \qquad (20)$$

And from the incremental theory:

$$\dot{W}' = 2\pi\, F\, R_o \cdot \sqrt{1+\zeta}\,\cos\alpha_o$$

$$+\sqrt{1+\zeta}\, R_o F \sin\alpha_o \int \left\{ \frac{R_u\cos\theta-(Fn\,\sin\alpha_o-\rho_o\cos\alpha_o)}{\sqrt{r_o^2-[R_u\cos\theta-(Fn\,\sin\alpha_o-\rho_o\cos\alpha_o)]^2}} - \frac{R_l\cos\theta-(Fn\,\sin\alpha_o-\rho_o\cos\alpha_o)}{\sqrt{r_o^2-[R_l\cos\theta-(Fn\,\sin\alpha_o-\rho_o\cos\alpha_o)]^2}}\, d\theta \right\}$$

Boundary of the area of contact

where: $$\zeta = \frac{2\pi\cos\theta(R\cos\theta-\beta)(\sqrt{\psi})^2 - r_o^2\sin\theta\,[2\pi R\sin\theta + F\sin\alpha_o]}{2\pi\sin\theta(R\cos\theta-\beta)(\sqrt{\psi})^2 - r_o^2\cos\theta\,[2\pi R\sin\theta + F\sin\alpha_o]}$$

$$\beta = Fn\sin\alpha_o - \rho_o\cos\alpha_o$$

$$\sqrt{\psi} = \sqrt{r_o^2 - [R\cos\theta - (Fn\sin\alpha_o - \rho_o\cos\alpha_o)]^2}$$

$$\dot{W} = \frac{\sigma_o S_o}{\sqrt{3}}\, N\, \dot{W}'$$

$$t' = \frac{\dot{W}'}{2\sqrt{3}\,\pi R}$$

$$t = \sigma_o\, S_o\, t'$$

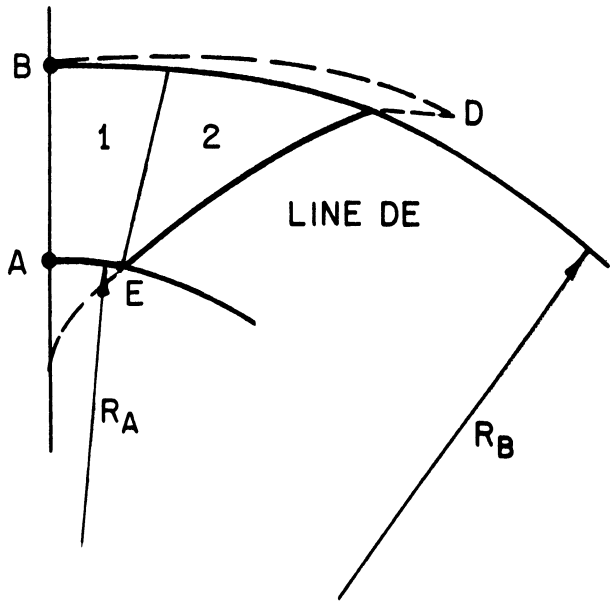

Fig. 15 - Approximated area of contact

For the integration, the boundaries of the area of contact are to be computed. Because the cylindrical portion of the roller is disregarded, area B is omited. Let the remained of the area of contact be approximated by the configuration of Fig. 15.

The integration will be done for Area 1 and for Area 2.

For area 1: $R_u = R_B = Fn \sin \alpha_o - \rho_o \cos \alpha_c$

$R_l = R_A = R_o$

$\theta_u = \theta_E$

$\theta_l = 0$

For area 2: $R_u = R_B = Fn \sin \alpha_o - \rho_o \cos \alpha_o$

$R_l = R_{ED}(\theta)$ = R of line ED as a function of θ

$\theta_u = \theta_D$

$\theta_l = \theta_E$

For simplicity (and to save drum locations on the computer), let R_l of area 2 be linearly dependent θ.

$$R_l = R_o + (R_B - R_o) \frac{\theta - \theta_l}{\theta_u - \theta_l}$$

To solve for θ_E and θ_D, one solves the equation of the torus:

$$G = 0$$

where:

$$Z = b + \sqrt{b^2 - C}$$

$$b = \rho_o \sin \alpha_o + F(n-1) \cos \alpha_o$$

$$C = (R \cos \alpha_o + \rho_o)^2 + \left[R \sin \alpha_o - F(n-1)\right]^2 - r_o^2$$

for θ when $R = R_o$ and when $R = R_B$, respectively. Newton's method of successive approximations will be used.

The equation $G(R,\theta) = 0$ is to be solved for R_o, for example. Thus $G(R_o,\theta) = 0$ is given; it is necessary to solve for θ. According to Newton's method:

$$\theta_1 = \theta_o - \frac{G(R_o\ \theta_o)}{G_o(R_o\theta_o)}$$

where θ_o is an approximation of the exact solution.

θ_1 is now closer to the exact solution of θ than θ_o is. If θ_o is replaced now by θ_1 and the computation is repeated, the solution approaches the exact value more and more closely. Repetition of the operation yields any desired accuracy.

Let:

$$G(\cos\theta) = \left[(R\cos\theta\cos\alpha_o - Z\sin\alpha_o)^2 + R^2(1-\cos^2\theta) - \rho_o \right]^2 + \left[R\cos\theta\sin\alpha_o + Z\cos\alpha_o - Fn\right]^2 - r_o^2 = 0$$

where: $Z = b + \sqrt{b^2 - C}$

$$b = \rho_o \sin\alpha_o + F(n-1)\cos\alpha_o$$

$$C = (R\cos\alpha_o + \rho_o)^2 + \left[R\sin\alpha_o - F(n-1)\right]^2 - r_o^2$$

$$\frac{\partial[G(\cos\theta)]}{\partial(\cos\theta)} = 2\left[(R\cos\theta\alpha_o - Z\sin\alpha_o)^2 + R^2(1-\cos^2\theta) - \rho_o\right] \cdot$$

$$\frac{(R\cos\theta\cos\alpha_o - Z\sin\alpha_o)\,R\cos\alpha_o - R^2\cos\theta}{\sqrt{(R\cos\theta\cos\alpha_o - Z\sin\alpha_o)^2 + R^2(1-\cos^2\theta)}}$$

$$+\ 2\left[R\cos\theta\sin\alpha_o + Z\cos\alpha_o - Fn\right] R\sin\alpha_o$$

The value of cos θ will be solved by Newton's method for any desired R.

$$\cos \theta_1 = \cos \theta_o - \frac{G(\cos \theta_o)}{\frac{\partial [G(\cos \theta_o)]}{\partial (\cos \theta_o)}}$$

Then the value of θ itself will be computed.

After solving for θ_E and θ_D, the program will solve for the value of ζ at these two points. The valve of ζ at θ_D will be used as a representative value for an average of ζ.

The integration of the terms under the integral is done by Simpson's rule for numeric integration.

As Fig. 12 shows, some work is done along the boundary CDEF, which is not included in the work of deformation under the area of contact. A direct computation of this work seems difficult. To account for this work, it was assumed that the additional work is proportional to the value of $\dot{\epsilon}_{\theta Z}$ and it has been added to the correcting factor under the root ($\sqrt{1+\zeta}$).

Let the equation for the main power be written as:

$$\dot{W}'_p = 2\pi F R_o \cdot \sqrt{1 + a \cdot \zeta} \cdot \cos \alpha_o$$

where a is a multiplying factor to account for the work at the boundary CDEF.

The "IT" language for an IBM 650 was used in this solution with the library sub-routines of The University of Michigan Statistical Research Laboratory.

Before presenting the program, the assignment list is given:

Table II - Assignment list for the results

C5 - R_o radius at point A

C6 - ρ_o roller radius

C7 - r_o Roller "round-off" radius

C8 - α_o Half included angle

C9 - F Feed per revolution

C10 - half the number of intervals used in Simpson integration

Y1 - $\dot{W}1$ Complementary weighted power at area 1

Y2 - $\dot{W}2$ Complementary weighted power at area 2

Y9 - $\dot{W}9$ Principal weighted power

Y11 - $\dot{W}11$ Total weighted power by the deformation theory

Y13 - t' Weighted tangential force by deformation theory

Y14 - t' Weighted tangential force by incremental theory

Y19 - $\dot{W}19$ Total weighted power by the incremental theory

I0 - Identification number for the set of parameters (see Table (4).)

I1 - Percent of Y1 of total power

I5 - Percent of Y2 of total power

I4 - Percent of Y4 total power

I9 - Percent of Y9 of total power

I17 - Percent of power by incremental theory to power by deformation theory

C110 - Cos θ_E

C111 - Cos θ_D

C113 - Strain-rates ratio γ at point E

C114 - Strain-rates ratio γ at point D

Table III - General Assignment List

C1 - R
C2 - θ } coordinates position in space
C3 - Z

C4 - N - Speed in rpm

C5 - R_o - Radius at point A

C6 - ρ_o - Roller radius

C7 - r_o - Roller "round-off" radius

C8 - α_o - Half the included angle of the cone

C9 - F - Feed in ipr

C10 - Half the number of intervals used in Simpson integration

C11 - Sin θ

C12 - cos θ

C13 - sin α_o

C14 - cos α_o

C23 - $\rho_o \cdot \sin \alpha_o$

C26 - F sin α_o

C27 - n - The number of revolution passed from time t = 0

C28 - F·n

C32 - $R \cos \theta \cos \alpha_o - Z \sin \alpha_o$

C33 - $\sqrt{(R \cos \theta \cos \alpha_o - Z \sin \alpha_o)^2 + R^2 \sin^2 \theta}$

C37 - $R \cos \theta \sin \alpha_o + Z \cos \alpha_o - Fn$

C42 - $(r_o + \rho_o) \cos \alpha_o$

C46 - $r_o + \rho_o$

C50 - θ_E, θ at the point E

C55 - $F(n-1) \cos \alpha_o$

C56 - $\rho_o \sin \alpha_o + F(n-1) \cos \alpha_o = b$

C57 - $F(n-1)$

C61 -
C62
C63 } Temporary variables used to compute the complementary power.
C64

C69 - $\rho_o \cos \alpha_o$

C72 - $R_B = Fn \sin \alpha_o - \rho_o \cos \alpha_o$

C73 - $R \cos \theta - (Fn \sin \alpha_o - \rho_o \cos \alpha_o)$

C74 - r_o^2

C75 - $r_o^2 - [R \cos \theta - (Fn \sin \alpha_o - \rho_o \cos \alpha_o)]^2$

C76 - $F \sin \alpha_o + 2\pi R \sin \theta$

C77 - $2\pi[R \cos \theta - (Fn \text{ Sin } \alpha_o - \rho_o \cos \alpha_o)] \cdot C75$

C78 - $(C77 * C11) + C74 * C12 * C76$

C79 - $(C77 * C12) - C74 * C11 * C76$

C80 - C79/C78

C83 - $C = (R \cos \alpha_o + \rho_o)^2 + [R \sin \alpha_o - F(n-1)]^2 - r_o^2$

C94 - $(C56 * C56) - C83$

C95 -
C96 - } Multiplying factors
C97 -

C100 - $\sqrt{\frac{1 - C111 * C111}{C111 * C111}}$

C101 - $G_{ED}(R,\theta,Z)$ The function G = 0 along line ED

C102 - $\frac{\partial [G_{ED}(R,\theta,Z)]}{\partial(\cos\theta)}$

C103 - C101/C102

C110 - $\cos\theta_E$

C111 - $\cos\theta_D$

C113 - ζ at point E, strain rates ratio at point E

C114 - ζ at point D, strain rates ratio at point D

C121 - $\rho_o \sin\alpha_o + F(n-1)\cos\alpha_o + r_o$

Y1 - $\dot{W}1$ - Complementary weighted power at area 1

Y2 - $\dot{W}2$ - Complementary weighted power at area 2

Y9 - $\dot{W}9$ - Principal weighted power

Y11 - $\dot{W}11$ - Total weighted power by the deformation theory

Y13 - t' - Weighted tangential force by the deformation theory

Y14 - t' - Weighted tangential force by the incremental theory

Y19 - $\dot{W}19$ - Total weighted power by the incremental theory

I0 - Identification number for the set of parameters (Table 4)

I1 - Percent of Y1 of total power

I2 - Alphabetic variable - "NOT"

I3 - Alphabetic variable - "GOOD"

I4 - Data for machine decission

I5 - Percent of Y2 of total power

I6 - Data for machine decission

I8 - Data for machine decission

I9 - Percent of Y9 of total power

I17 - Percent of power by incremental theory to power by deformation theory

TABLE IV

IDENTIFICATION NUMBER (IO) KEY

$\rho_o \equiv$ C6		$\alpha_o \equiv$ C8			F ≡ C9		$r_o \equiv$ C7		$R_o \equiv$ C5	
Radius, in.	Code	Degrees	Code	Radians	Feed	Code	Radius, in.	Code	Radius, in.	Code
1	01	15	15	0.26179900	.015	15	1/16 = .0625	01	1	01
2	02	21	21	0.36651900	.020	20	2/16 = 1/8 = .125	02	2	02
3	03	30	30	0.52359900	.021	21	3/16 = .1875	03	3	03
4	04	31.5	31	0.54977900	.030	30	4/16 = 1/4 = .250	04	4	04
5	05	35	35	0.61086500	.035	35	5/16 = .3125	05	5	05
6	06	42.5	42	0.74176600	.039	39	6/16 = 3/8 = .375	06	6	06
7	07	45	45	0.78539800	.040	40	7/16 = .4375	07	7	07
8	08	54	54	0.94247800			8/16 = 1/2 = .5	08	8	08
9	09	60	60	1.04719800					9	09
10	10	75	75	1.30899600					10	10

Example:

The variables: ρ_o = 7 in., α_o = 35°, F = .025 ipr, r_o = 1/4 in., R_o = 5 in.

The code: IO = 07 35 25 04 05

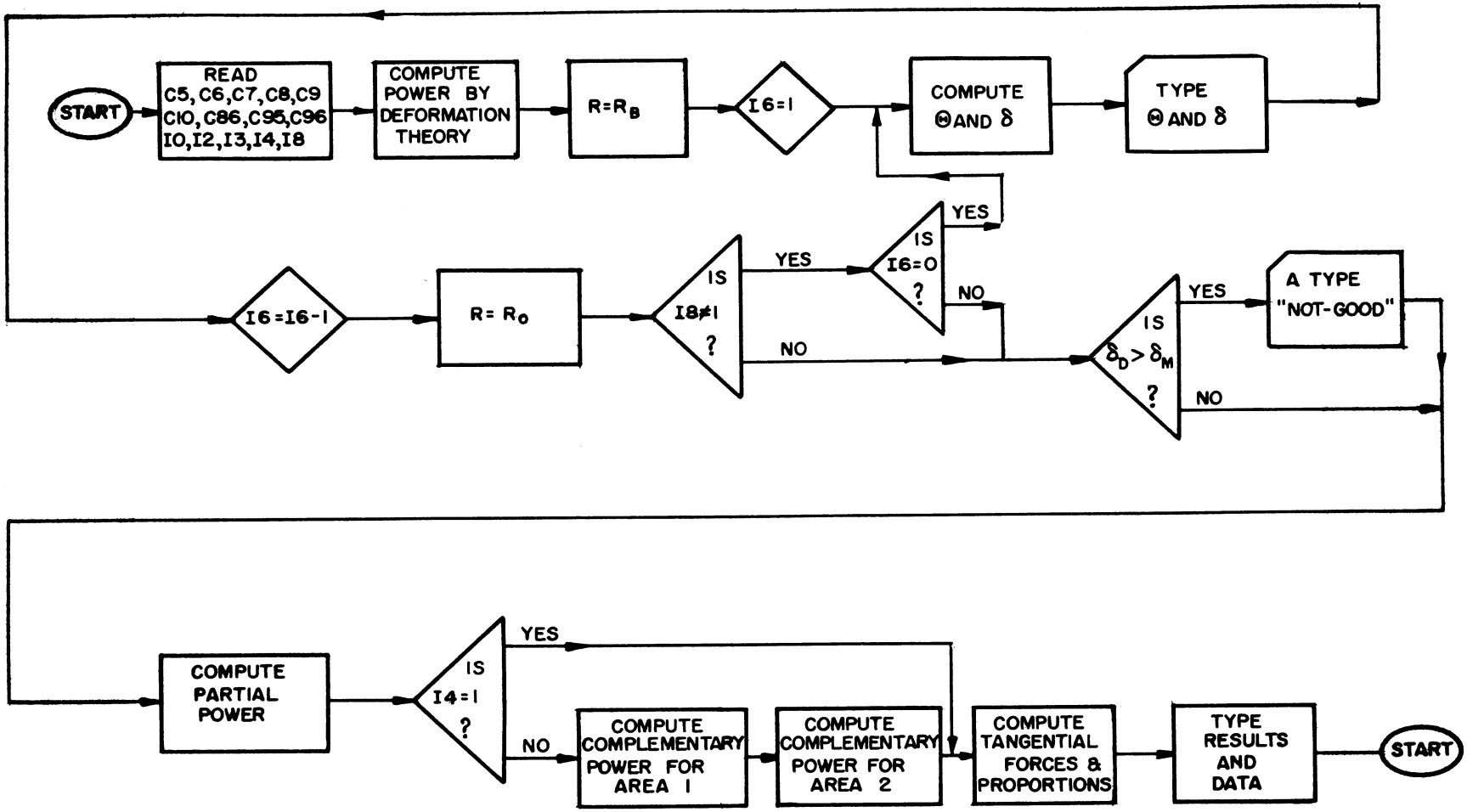

δ – STRAIN – RATE RATIO AT THE POINT DEFINED BY R AND θ

δ_M – CRITICAL VALUE OF δ

δ_D – δ AT POINT D

Fig. 27 – Flow diagram for the computer program

Program for Power and Tangential Force

```
0007        I0,C5...C10,C86 READ                    F
            C13=Q22EKC8Q                            F
            C14=Q21EKC8Q                            F
            C23=C6*C13                              F
            C69=C6*C14                              F
            C46=C6+C7                               F
            C26=C9*C13                              F
            C42=C46*C14                             F
            C27=(C5+C42)/C26                        F
            C28=C9*C27                              F
            C57=C9*(C27-1.)                         F
            C55=C57*C14                             F
            C56=C55+C23                             F
            C121=C56+C7                             F
            C72=(C28*C13)-C69                       F
            Y11=6.2831853*C5*C9*C14                 F
            C1=C72                                  F
            I6=1                                    F
0006        C12=.99                                 F
            C83=((C6+C1*C14)*C6+C1*C14)+((
            C57-C1*C13)*C57-C1*C13)-C7*C7F
            C94=(C56*C56)-C83                       F
            G22IFC94V0.                             F
            C94=0.                                  F
0022        C3=C56+Q20EKC94Q                        F
0015        C32=(C1*C12*C14)-C3*C13                 F
            C33=Q20EK((C32*C32)+C1*C1*(1.-
            C12*C12))Q                              F
            C37=(C1*C12*C13)+(C3*C14)-C28F
            C101=((C33-C6)*(C33-C6))+(C37*
            C37)-C7*C7                              F
            C102=2.*(((C33-C6)*(C32*C1*C14
            )-C1*C1*C12)/C33)+C1*C13*C37 F
            C103=C101/C102                          F
            C12=C12-C103                            F
            G15IFAC103WC86                          F
            C(110+I6)=C12                           F
            C73=(C1*C12)-C72                        F
            C11=Q20EK(1.-C12*C12)Q                  F
            C74=C7*C7                               F
            C75=C74-C73*C73                         F
```

```
                C76=C26+6.283*C1*C11                F
                C77=6.283*C73*C75                   F
                C78=(C77*C11)+C74*C12*C76           F
                C79=(C77*C12)-C74*C11*C76           F
                C80=C79/C78                         F
                C(113+I6)=C80*C80                   F
0011            TI0TC(113+I6)TC(110+I6)             F
                I6=I6-1                             F
                C1=C5                               F
                G14IFI8U1                           F
                G6IFI6U0                            F
0014            G3IFAC114WC95                       F
0020            Y9=Y11*(Q20EK(1.+C96*C114)Q)        F
                G19                                 F
0003            ATI2TI3                             F
                G20                                 F
0019            G18IFI4U1                           F
                C12=Q20EK((1.-C12*C12)/C12*C12
                )Q                                  F
                C50=Q23EKC12Q                       F
                C3=Q27EK0.KC50KC10K1K2K9Q           F
0002            C12=Q21EKC3Q                        F
                C61=(C5*C12)-C72                    F
                C62=(C7*C7)-C61*C61                 F
                C62=AC62                            F
0004            C63=C61/(Q20EKC62Q)                 F
                C61=C72*C12-1.                      F
                C62=(C7*C7)-C61*C61                 F
                C62=AC62                            F
0005            C64=C61/(Q20EKC62Q)                 F
                Y1=C5*C9*C13*C64-C63                F
                G2                                  F
0009            Y1=Y1*(Q20EK(1.+C96*C114)Q)         F
                C100=Q20EK((1.-C111*C111)/C111
                *C111)Q                             F
                C101=Q23KC100Q                      F
                C3=Q27EKC50KC101KC10K2K10K16QF
0010            C12=Q21EKC3Q                        F
                C61=C5-C72+(C72-C5)*C12*(C3-C5
                0)/(C101-C50)                       F
                C62=(C7*C7)-C61*C61                 F
```

```
                C62=AC62                                F
                C63=C61/(Q20EKC62Q)                     F
                C61=C72*C12-1.                          F
                C62=(C7*C7)-C61*C61                     F
                C62=AC62                                F
                C64=C61/(Q20EKC62Q)                     F
                Y2=C5*C9*C13*C64-C63                    F
                G10                                     F
0016            Y2=Y2*(Q20EK(1.+C96*C114)Q)             F
0018            Y19=AY1+AY2+AY9                         F
                I17=100.*Y19/Y11                        F
                Y13=.5*Y11/1.73205*3.14159*C5F
                Y14=.5*Y19/1.73205*3.14159*C5F
                G23IFI4U1                               F
                I1=100.*Y1/Y19                          F
                I5=100.*Y2/Y19                          F
                I9=100.*Y9/Y19                          F
0012            TIOTY1TY2TY9TY19                        F
0008            TIOTI1TI5TI9                            F
0023            TIOTC5TC6TC7TC8                         F
0001            TIOTC9TC10TC86TC96                      F
0021            TIOTC95TI4TI8TI17                       F
0013            TIOTY11TY9TY13TY14                      F
0017            TIOTC50TC101                            F
                G7                                      F
                H                                      FF
```

COMPARING THE STRAIN RATES

```
0007        I0,C5...C10,C86 READ                F
            C13=Q22EKC8Q                        F
            C14=Q21EKC8Q                        F
            C23=C6*C13                          F
            C69=C6*C14                          F
            C46=C6+C7                           F
            C26=C9*C13                          F
            C42=C46*C14                         F
            C27=(C5+C42)/C26                    F
            C28=C9*C27                          F
            C57=C9*(C27-1.)                     F
            C55=C57*C14                         F
            C56=C55+C23                         F
            C72=(C28*C13)-C69                   F
            I6=5                                F
            C43=(C72-C5)/5.                     F
0001        C1=C72-I6*C43                       F
0006        C12=.99                             F
            C83=((C6+C1*C14)*C6+C1*C14)+((
            C57-C1*C13)*C57-C1*C13)-C7*C7F
            C94=(C56*C56)-C83                   F
            G22IFC94V0.                         F
            C94=0.                              F
0022        C3=C56+Q20EKC94Q                    F
0015        C32=(C1*C12*C14)-C3*C13             F
            C33=Q20EK((C32*C32)+C1*C1*(1.-
            C12*C12))Q                          F
            C37=(C1*C12*C13)+(C3*C14)-C28F
            C101=((C33-C6)*(C33-C6))+(C37*
            C37)-C7*C7                          F
            C102=2.*(((C33-C6)*(C32*C1*C14
            )-C1*C1*C12)/C33)+C1*C13*C37        F
            C103=C101/C102                      F
            C12=C12-C103                        F
            G15IFAC103WC86                      F
            C(105+I6)=C12                       F
            C73=(C1*C12)-C72                    F
            C11=Q20EK(1.-C12*C12)Q              F
            C74=C7*C7                           F
            C75=C74-C73*C73                     F
            C76=C26+6.283*C1*C11                F
            C77=6.283*C73*C75                   F
            C78=(C77*C11)+C74*C12*C76           F
            C79=(C77*C12)-C74*C11*C76           F
            C80=C79/C78                         F
            C(113+I6)=C80*C80                   F
```

```
0002        TIOTC(113+I6)TC79TC78TC(105+I6
0002        )                                F
            I6=I6-1                          F
            I7=I6+1                          F
            G3IFI7U0                         F
            G1                               F
0003        I6=1                             F
            C43=(1.-C105)/5.                 F
            C1=C72                           F
            C12=1.                           F
0004        C73=(C1*C12)-C72                 F
            C11=Q20EK(1.-C12*C12)Q           F
            C74=C7*C7                        F
            C75=C74-C73*C73                  F
            C76=C26+6.283*C1*C11             F
            C77=6.283*C73*C75                F
            C78=(C77*C11)+C74*C12*C76        F
            C79=(C77*C12)-C74*C11*C76        F
            C80=C79/C78                      F
            C(118+I6)=C80*C80                F
0005        TIOTC(118+I6)TC79TC78TC12        F
            C12=C12-C43                      F
            I6=I6+1                          F
            G4IFC12WC105                     F
            G7                               F
            H                               FF
```

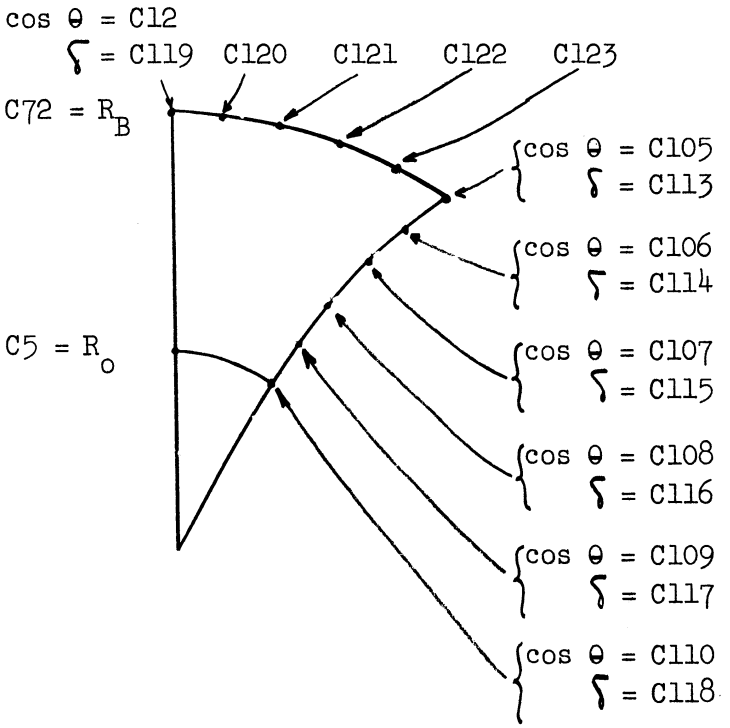

APPENDIX 2

COMPARING THE TANGENTIAL FORCES FOR SHEAR AND BENDING

The type of deformation that takes place can be assumed as bending or shear, as will be explained immediately. The actual deformation can be anything between these two types (see Fig. 19).

A. BEND

Each point on the central surface remains at its previous radial distance (R) from the axis Z. The straight lines AB and CD remain straight and perpendicular to the surface. AB becomes A'B' and CD becomes C'D'. The length $A'B' = AB \sin \alpha_o$.

B. SHEAR

Shear was described earlier (Fig. 5). Each point remains at its previous distance (R) from the center (Z axis). The straight lines AB and CD remain straight with no change in length. However, in this case they are no longer perpendicular to the surface, but parallel to the Z axis.

Let the tangential force be computed with the deformation theory. For shear deformation the tangential force was found to be:

$$t_s = \frac{S_o \sigma_o}{\sqrt{3}} F \cos \alpha_o$$

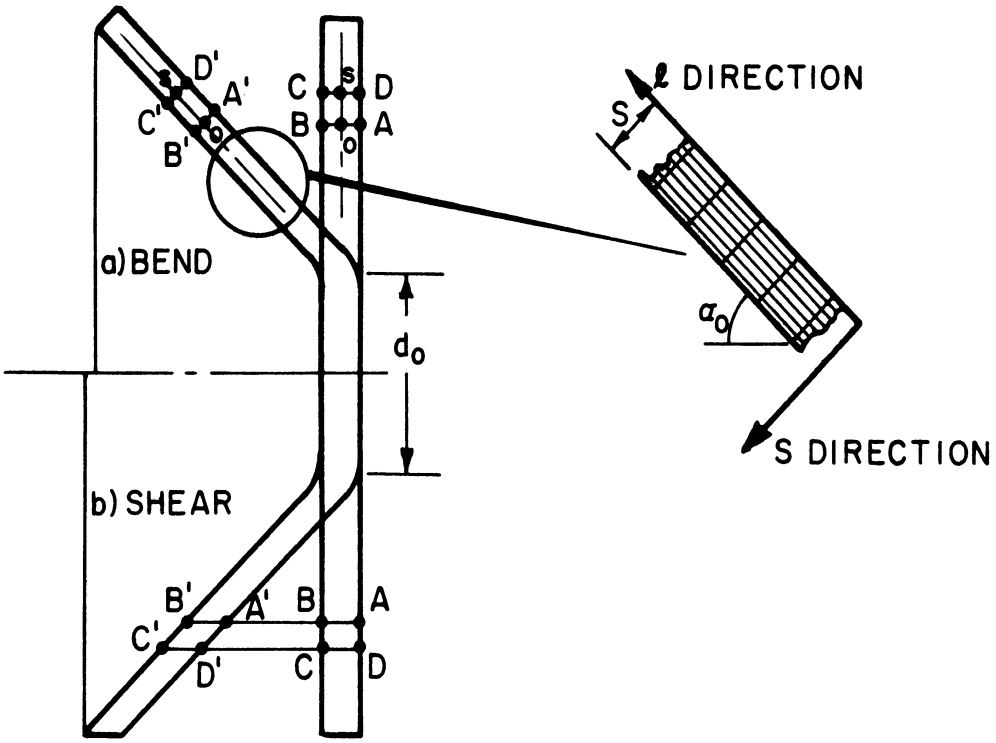

Fig. 19 - The shear & bending strains

For pure bending the steps are as follows:

Let the power be:

$$\dot{W} = V \int \bar{\sigma}_o d\phi = V\sigma_o \phi$$

where: V is the volume deformed per minute
σ_o the yield limit under uniaxial tension
ϕ the effective logaritmic strain

Let ϕ_θ be the circumferential logarithmic strain at the middle surface
ϕ_S be the width avg. logarithmic strain
ϕ_1 be the length logarithmic strain (see Fig. 19)

The middle surface has no circumferential change in length, and therefore

$$\phi_\theta = 0$$

The thickness is reduced from S_o to $S_1 = S_o \sin \alpha_o$

and therefore: $$\phi_S = \ln \frac{S_1}{S_o} = \ln (\sin \alpha_o)$$

From the volume constancy, one gets

$$\phi_1 = -\phi_S - \phi_\theta = -\phi_S$$

The definition of the effective strain in the absence of shear strains

$$\phi = \frac{2}{3}\sqrt{\frac{1}{2}\left[(\phi_\theta - \phi_1)^2 + (\phi_1 - \theta_S)^2 +)\phi_S - \phi_\theta)^2\right]}$$

in this case reduces to

$$\phi = \frac{2}{3}\sqrt{\frac{1}{2}(\phi_S^2 + 4\phi_S^2 + \phi_S^2)} + \frac{2}{\sqrt{3}}\phi_S = \frac{2}{\sqrt{3}} \ln (\sin \alpha_o)$$

The volume deformed per minute is:

$$V = 2\pi RN\, S_o\, \Delta R = 2\pi RN\, S_o\, F \sin \alpha_o$$

And thus:

$$\dot{W} = 2\pi RN\, S_o\, F \sin\alpha_o\, \sigma_o \cdot \frac{2}{\sqrt{3}} \cdot \ln(\sin\alpha_o)$$

And the tangential force

$$t_c = \frac{\dot{W}}{2\pi RN} = 2 \cdot S_o \cdot \frac{\sigma_o}{\sqrt{3}} F \sin\alpha_o \cdot \ln(\sin\alpha_o)$$

For comparison purposes let a weighted tangential force be defined such that

$$t' = \frac{t \cdot \sqrt{3}}{S_o \cdot \sigma_o}$$

The bending assumption gives

$$t_c' = 2F \sin\alpha_o \ln(\sin\alpha_o)$$

The shear assumption gives

$$t_S' = F \cos\alpha_o$$

Figure 20 describes the weighted tangential force for a feed of .100 ipr for half included angle from $\alpha_o = 0$ to $\alpha_o = 90^o$.

APPENDIX 3

EVALUATING THE YIELD LIMIT

In the analytical approach, Mises material was considered. The characteristics of the material were thus presented by a single value of the yield limit (σ_o). Actual materials, however, have an elastic range as well as a strain-hardening effect. The most convenient way to present the characteristics of an actual material is by its tensile test recording of a uniaxial stress

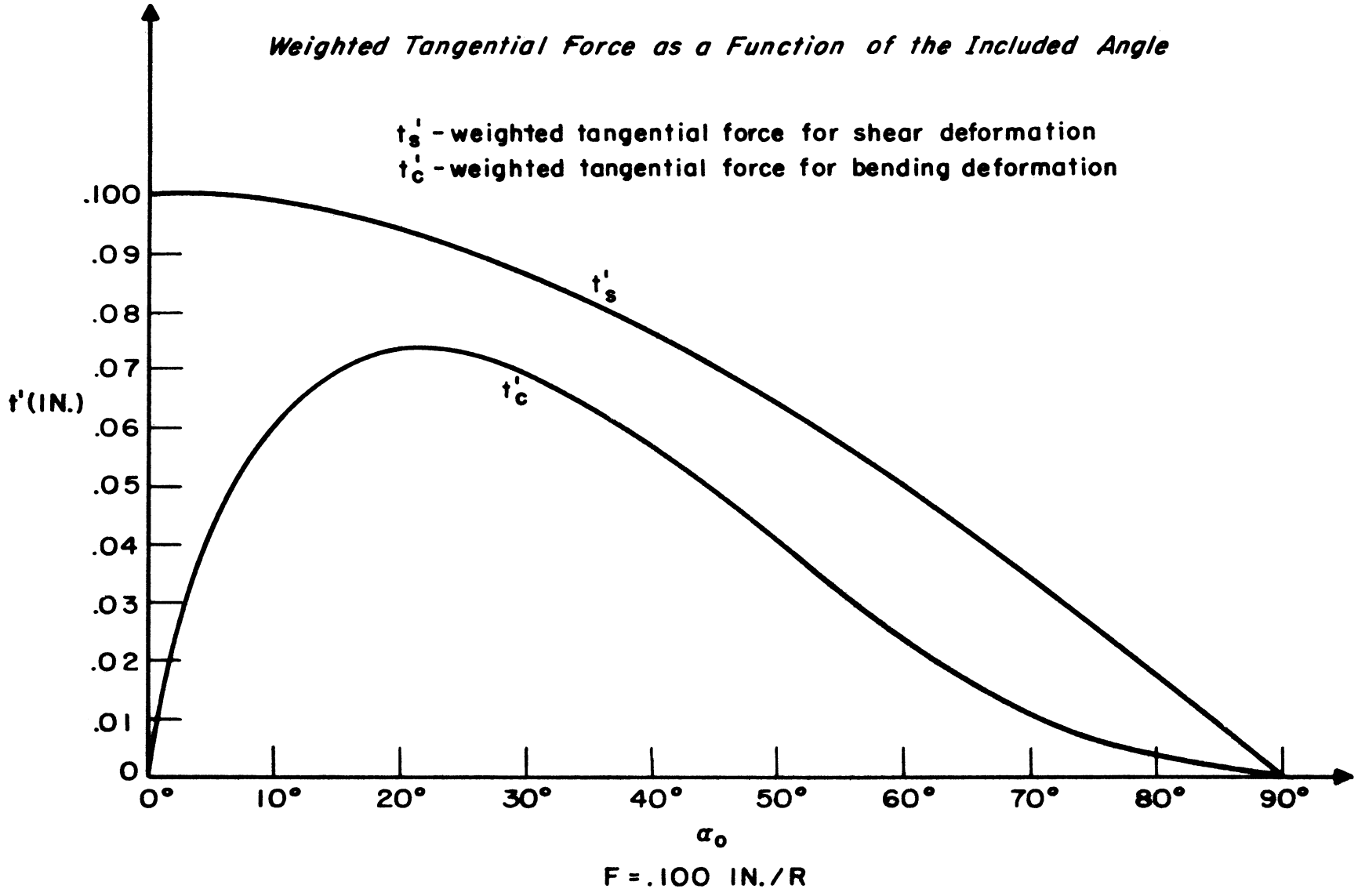

Fig. 20 - Comparing shear deformation to bending

plotted against the strain. For the check of the numerical answer against the experimental power consumed, a representative value for σ_o is to be chosen from the tensile test recording.

First, the question of the elastic portion of the deformation was considered. Steel with modulus of elasticity of 30,000,000 $lb/inch^2$ and with extremely high yield limit of σ_o = 80,000 $lb/inch^2$ will serve as an example. For this particular material, the strain at yield with uniaxial stress will be

$$\epsilon_{yield} = \frac{80,000}{30,000,000} < .003$$

Let the shear at 45^o to the principal axis be found for this case. The shear stress $\tau = \frac{\sigma_o}{2}$

The shear strain is $\gamma = \frac{(1+\nu)}{E}\tau \approx \frac{1.5}{2} \cdot \frac{\sigma_o}{E} \approx .0022$

Transferring the radians to degrees, one gets maximum shear in the elastic range of $.13^o$ for original angle of 90^o.

The shear strain at yield is much smaller than the minimum shear (5^o) considered in this study. Considering this elastic deformation as part of the plastic deformation has no effect on the numerical results. This is clearly illustrated in Fig. 28 where a stress-strain curve of an actual tensile test is recorded at constant speed of the chart.

From the actual recording an average value was picked up and denoted to be the representative yield limit σ_o. The value of σ_o is neither far from the minimum nor from the maximum value of the stress on the chart.

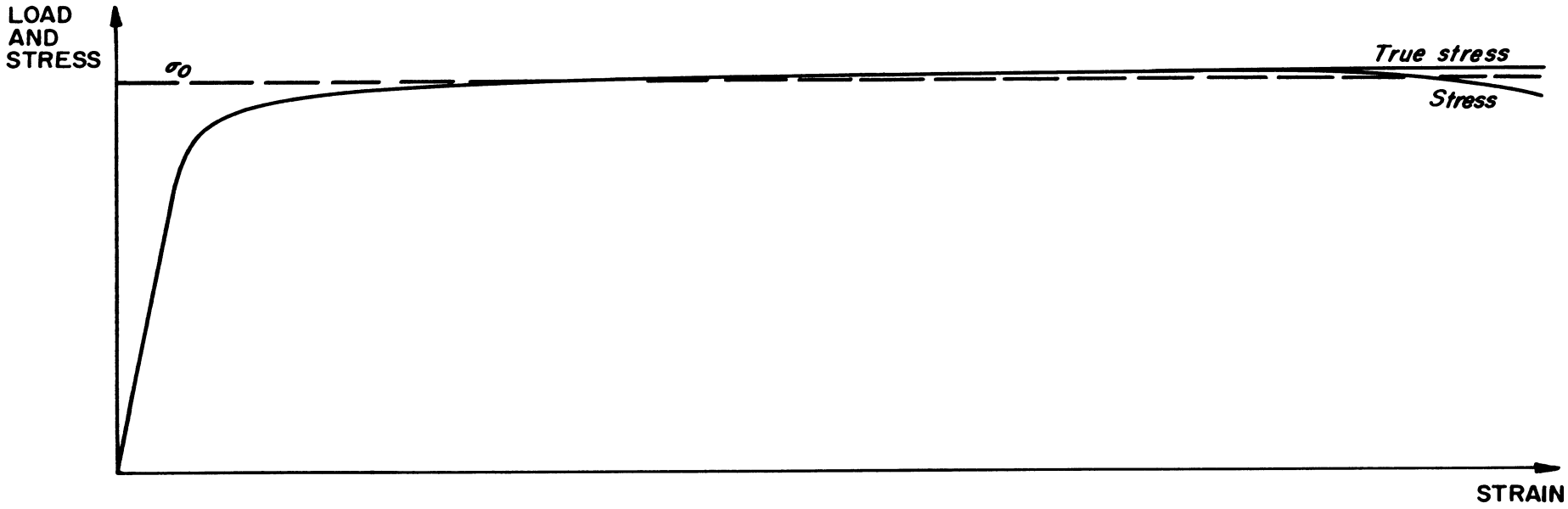

Fig. 28-Stress strain curve for Al.